ELECTROCHEMICAL EVALUATION OF SELF-HEALING EPOXY COATED REBAR IN SIMULATED CONCRETE PORE SOLUTION

A Thesis

by

REECE KEITH GOLDSBERRY

Submitted to the Office of Graduate and Professional Studies of
Texas A&M University
in partial fulfillment of the requirements for the degree of

MASTER OF SCIENCE

Chair of Committee,	Homero Castaneda-Lopez
Co-Chair of Committee,	Raymundo Case
Committee Members,	Zenon Medina-Cetina
Head of Department,	Ibrahim Karaman

May 2019

Major Subject: Materials Science and Engineering

ABSTRACT

The use of epoxy-coated rebar (ECR) has become a major form of protection for reinforcing steel in concrete bridges in North America. ECR has been shown to increase the service life of reinforced structures but a few structures showed severe corrosion of the rebar when the coating had been previously damaged or in the presence of high chloride concentrations. The increase of protectiveness from the addition of microcapsules containing triethanolamine (TEA) in the presence of chlorides is studied. The microcapsules containing TEA were produced by free radical polymerization and involving a 4-step process. When the coating has been damaged the microcapsules can release TEA either due to mechanical rupturing or when there is a local pH difference due to the corrosion of the rebar. To test the corrosion inhibition effect of the admixed microcapsules the coating is damaged to accelerate the corrosion of the rebar. Electrochemical corrosion testing and visual inspection were performed to determine the effect of the addition of microcapsules on the damaged coatings protection. A carbonated simulate pore solution was chosen for electrochemical testing to simulate an aggressive environment to initiate the corrosion process to promote the release of the corrosion inhibitor. Electrochemical impedance spectroscopy, linear polarization resistance, open circuit potential, and scanning vibrating electrode technique were the electrochemical tests performed to characterize the interfacial reactions under corrosive environment. The addition of microcapsules to the epoxy coating showed a corrosion inhibition effect for the damaged coating. This can be seen by a delay in the time for the exposed area to become fully corroded for samples exposed to electrochemical testing and exposed in an accelerating fog chamber. Also, the samples with the addition of microcapsules showed larger values of the polarization resistance (Rp) for the duration of testing, but all samples showed a decrease in the Rp with exposure, which is due to corrosion occurring in the exposed area.

ACKNOWLEDGEMENTS

I would like to thank my committee chair, Dr. Castaneda, my co-chair Dr. Raymundo, and committee member, Dr. Medina-Cetina for their guidance and help throughout my time working on my research.

I would also like to thank Dr. Karayan for his support and help over the course of this research.

Also, a thank you to my girlfriend, friends and family for their constant encouragement and support.

CONTRIBUTORS AND FUNDING SOURCES

Contributors

This work was supervised by a thesis committee consisting of Professor Homero Castaneda and Professor Raymundo Case of the Department of Materials Science and Engineering and Professor Zenon Medina-Cetina of the Department of Civil Engineering.

TEA microcapsules were produced by Dr. Jose Milla from Louisiana Department of Transportation and Development.

All other work conducted for the thesis was completed by the student independently.

Funding Sources

Graduate study was supported by a fellowship from Texas A&M University and a dissertation research fellowship from Transportation Consortium of South-Central States Department of Transportation project Ni Louisiana State University.

Its contents are solely the responsibility of the authors and do not necessarily represent the official views of the Transportation Consortium of South-Central States Department of Transportation.

NOMENCLATURE

ECR	Epoxy-Coated Rebar
TEA	Triethanolamine
EIS	Electrochemical Impedance Spectroscopy
LPR	Linear Polarization resistance
OCP	Open Circuit Potential
SVET	Scanning Vibrational Electrode Technique
EDL	Electrical double layer

TABLE OF CONTENTS

LIST OF FIGURES

Page

LIST OF TABLES

Page

1. INTRODUCTION

Corrosion of reinforcing steel is a major concern to new and existing structures, since the degradation of the reinforcing steel will cause the premature failure of reinforced structures. A recent cost-of-corrosion study by the Federal Highway Administration has estimated the annual cost of corrosion to USA bridges to be approximately $30 billion, not including indirect costs incurred by the traveling public due to infrastructural closures [1]. The corrosion process on the rebar can be initiated by either a reaction with the environment (carbonation), pollution, or a diffusion of aggressive ions (chlorides). For marine environments and places where de-icing salts are used, the leading cause of corrosion is due to the ingress and buildup of chloride ions at the rebar/concrete interface. The corrosion model proposed by Tuutti [2], separates the corrosion process into two periods: initiation and propagation.

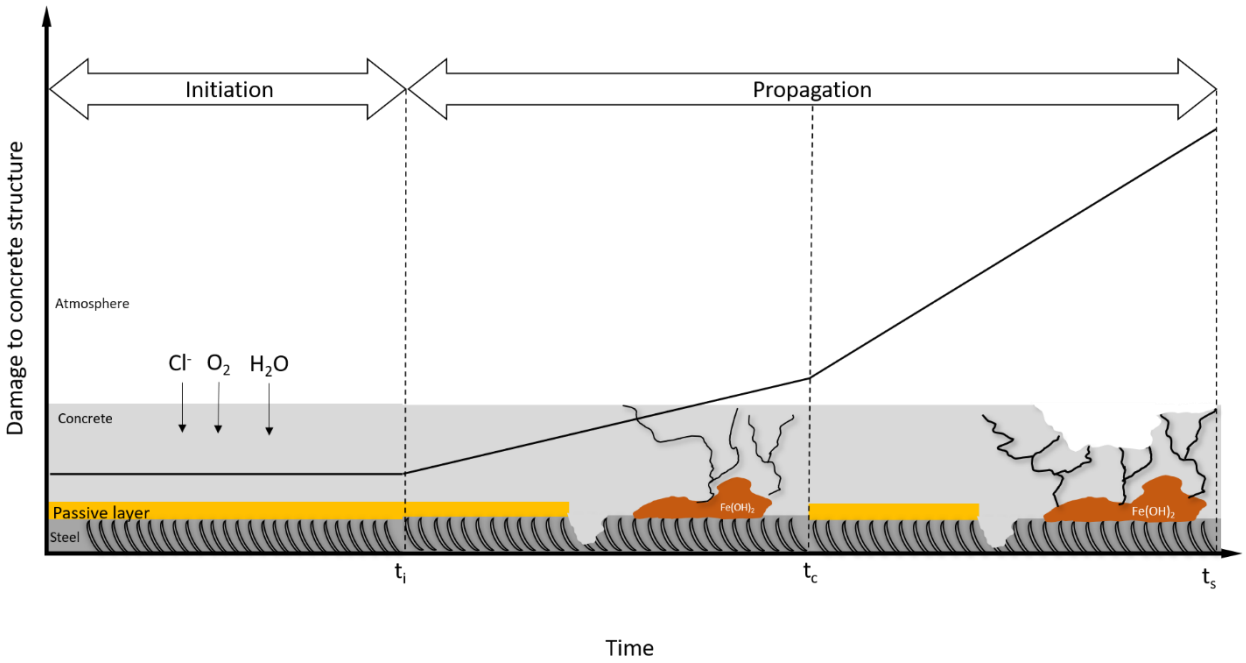

Figure 1: Service life of reinforced concrete structure

Initiation period refers to the ingress of aggressive ions and carbonation process to initiate the corrosion on the rebar. Propagation period is the time after corrosion process has occurred on the rebar, and is dominated by the kinetics of the system. Figure 1 shows the timeline of the corrosion process and damage of the reinforced structure for an unprotected rebar. Where t_i is the time of initiation of the corrosion process on rebar, t_c is the time that cracking is noticed on the surface of the reinforced structure, and t_s is the time that spalling has occurred. The initiation time depends on quality of concrete, concrete cover, corrosion prevention methods, and surrounding environment. To increase the service life of the rebar higher quality concrete and corrosion prevention methods are used to increase the initiation time of corrosion on the reinforcing steel. The time that cracking is noticed on the surface and time to spalling is dependent on the speed of the corrosion process which depends on the kinetics of the system.

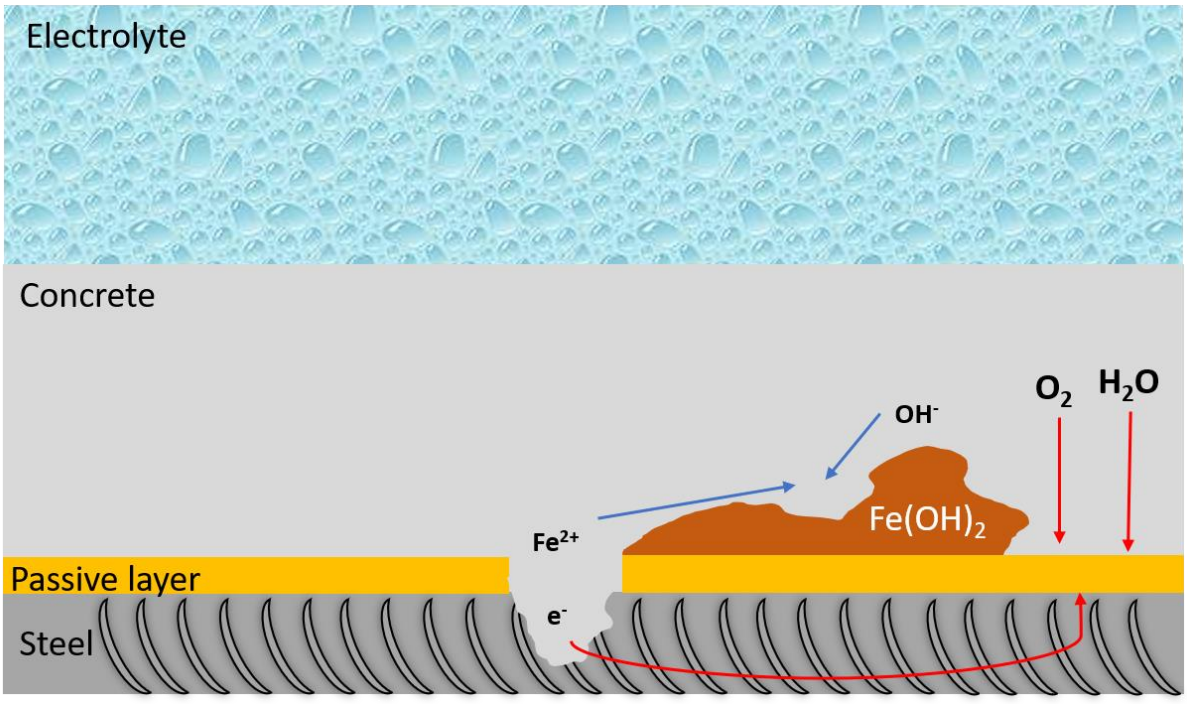

Figure 2: Corrosion process in reinforced concrete

Figure 2 shows an overview of the corrosion process of steel in concrete environment. Initially the rebar is in a passive state that protects the rebar from corrosion. This passive layer is due the high alkalinity of local environment, with pH values ranging from 12.5-14 depending on the properties and age of the concrete [3]. The passive layer that is formed on the rebar can be destroyed either by a drop in the local pH or from the buildup of aggressive ions in a localized area. The drop in the local pH is due to carbonation of the concrete. Carbonation is the reaction of CO_2 with water to form carbonates (CO_3^{2-}) and bicarbonates (HCO_3^-). The presence of these ions will lower the pH of the pore solution as long as there are enough carbonates present [4]. Carbonation will not only affect the pH of the environment but can also change the structure of the concrete matrix with the formation of carbonation bi-products ($CaCO_3$). From the carbonation process the pH will be around 8.5 compared to 12.5-14 for fresh uncarbonated concrete [3]. When the pH drops this low there will no longer be passive layer there to protect the rebar allowing the initiation of corrosion. The corrosion of reinforcing steel can also be initiated when a critical chloride concentration has been surpassed which breaks down the passive layer [5, 6]. Chlorides have a fourfold negative effect on concrete such as: destroys the passive film of the steel, reduces the pH of the pore water, increases the ion diffusion coefficient, and increases the electrical conductivity of the concrete [4].Once the passive layer is destroyed either due to carbonation or chloride diffusion or a combination of the two the corrosion process will begin, where the anodic and cathodic reactions are [7]:

$$\text{Anodic: } Fe \rightarrow Fe^{2+} + 2e^- \quad (1)$$

$$\text{Cathodic: } 2H_2O + O_2 + 4e^- \rightarrow 4OH^- \quad (2)$$

The iron ions released from the anodic process will form corrosion products of ferrous hydroxide ($Fe(OH)_2$) and ferric hydroxide ($Fe(OH)_3$), and hydrated ferric oxide ($Fe_2O_3 * H_2O$) [7].

During the corrosion process the iron ions can either react at the anodic site or travel through the pore system further into the concrete to react. The corrosion products will produce an expansive force due to the corrosion products having a volume that is 4 to 6 times larger relative to iron [7, 8]. This expansive force can crack the concrete forming a direct path for water diffusion, lower the strength of the concrete, and create spalling of the concrete. Once cracking or spalling has occurred then the reinforced structure must be repaired to prevent the failure of the structure.

Improving the ways to increase the service life of reinforced concrete structures is a continuing process. An abundance of research has been performed on how to further protect the rebar and to extend the service life of reinforced concrete structures such as:

- Improving quality of concrete
- Cathodic Protection
- Coating the outside surface of the structure
- Admixtures of corrosion inhibitor in the concrete matrix
- Epoxy, metallic, and polymeric coatings on the rebar

The cathodic protection (CP) of rebar can provide protection to existing and new structures. There are two forms of CP that can be used on reinforced structures, impressed current and galvanic anodes. The consideration of anode placement, amount of current needed and the type of CP system must be taken into account when using a CP system. The design and implementation would be different for new and existing structures. Some negative aspects of impressed current CP are: concrete degradation, adhesion loss at rebar/concrete interface, and hydrogen embrittlement [9]. For galvanic anode systems some negative aspects could be: no way to provide variable protection with a dynamic environment, anode corrodes to quickly and does not provide protection long enough. The effectiveness of CP systems is very environment

dependent, and if during the service life of the reinforced structure the environment varies to much then the system could not provide enough current to provide protection or could damage the structure with too much current. Surface coatings applied to reinforced concrete structures are able to be used on new and existing structures, as well as damaged structures. Due to the large variety of coatings available on the market choosing the right coating is critical. Some of the major things to account for in a coating are: diffusion coefficient, reactivity to certain chemicals, and durability. Due to this surface coatings can be very useful if the right coating is chosen or detrimental to the structure if the wrong coating is used. Surface coatings require regular maintenance to ensure the coating is intact and working properly, making this form of protection relatively high maintenance. The addition of corrosion inhibitors into the concrete matrix is known the increase the service life of reinforced structures [10, 11]. Corrosion inhibitors (CI) can either be added during mixing of the concrete for new structures, or applied to the surface of new and existing structures known as migrating corrosion inhibitors. The addition of corrosion inhibitor to the concrete can have varying effects on certain properties such as: chloride diffusion, compressive strength, air content, slump, heat of hydration, and workability [12, 13]. For corrosion inhibitor that are applied to the surface of hardened or curing concrete, it is difficult to know when and if the corrosion inhibitor has reached the rebar and once it has reached that there is a high enough concentration to protect the rebar. If there is not a high enough ratio of corrosion inhibitor to aggressive ions then small areas of corrosion can form since there is not enough corrosion inhibitor to protect the entire structure. This could lead to high corrosion rates in the localized area and further problems for the reinforced structure.

Epoxy coated rebar (ECR) has been used since the 1970's to provide protection for bridges [14]. ECR has been shown to provide ample protection when the rebar/coating are

handled properly, but when in the presence of high chloride concentration or damage has occurred to the coating this can lead to severe corrosion of the rebar [15]. Since the use of ECR began in the 1970s, ECR has been used in over 20,000 reinforced concrete bridge decks [16]. ECR is also commonly used in the construction of parking and marine structures, as well as in pavement. The use of ECR is a low cost and low maintenance form of corrosion protection for reinforced concrete structures compared to other corrosion protection methods. ECR must follow ASTM A775/ A775M-17: Standard Specification for Epoxy-Coated Steel Reinforcing Bars, which sets limits for: coating thickness, bending of the coating around a standard mandrel should not crack the coating, number of defects should not go above 6 per meter, and damaged area must not exceed 2% [17]. As with all corrosion protection systems there are advantages and disadvantages. A major advantage of an epoxy coating on the rebar is the denial of charged species due to the dielectric properties of the coating [7]. The epoxy coating can also provide a barrier that blocks water and oxygen from reaching the rebar, which will not allow the cathodic and anodic reactions to occur. The dielectric and barrier properties of the coating will delay the initiation time of corrosion on the rebar. Another advantage is that the use of ECR instead of uncoated rebar will not have a major impact on the design of the concrete structure compared to using other corrosion protection methods. The monitoring of the ECR with electrical and electrochemical methods is more difficult due to the insulating properties of this epoxy coating. Special care must be taken into account during the fabrication, transport, and pouring of concrete because this could cause mechanical damage to the coating exposing the rebar. Due to the stringent conditions for the fabrication of ECR there are only a limited number of factories that are certified to produce ECR for the use of construction. Once the coating is damaged severe corrosion will occur in the area where the damage has occurred due to the formation of a small

anode (damaged coating) and large cathode (undamaged coating). There is also a chance that once the corrosion process begins there can be undercutting surrounding the area of damaged coating. Undercutting in the corrosion process occurring on the substrate underneath the undamaged coating next to the damaged coating area. This could lower the adhesion strength of the coating to the rebar and the adhesion of the rebar/coating to the concrete.

A possible way to extend the life of the coating would be to use an epoxy coating that can protect the substrate after damage has occurred either mechanically or from water uptake. The addition of corrosion inhibitors directly into the epoxy matrix is a possible way to extend the service life and provide better corrosion resistance. There are a couple of drawbacks of adding corrosion inhibitors directly to the coating matrix. First, when using a corrosion inhibitor that is highly soluble the corrosion inhibitor would react before providing any long-term protection for the substrate. Also, there is a possibility that the corrosion inhibitor could create problems with the adhesion of the coating to the substrate if to soluble. On the other hand, if the corrosion inhibitor has to low of solubility it would not be able to provide ample protection to the substrate due to a lack of corrosion inhibitors at the substrate.

To delay the release of corrosion inhibitors or to release the corrosion inhibitors when the coating has become damaged the use of corrosion inhibitors encapsulated in polymeric microcapsules can be used. The release of the corrosion inhibitor from the microcapsule can be due to different mechanisms. These mechanisms are: diffusion through the polymeric shell, and mechanical rupturing or chemical breakdown of the polymeric shell. Triethanolamine (TEA) was chosen as the filler material for the microcapsules due to it being an organic amine corrosion inhibitor. Organic amine corrosion inhibitors have been widely used for corrosion protection of metal from aggressive environments due to their economic and effective corrosion retarding

capability in various industrial fields [18]. The chemical formula for TEA is $C_6H_{15}NO_3$ with a molecular weight of 149.19 g/mol and it is an organic tertiary amine and triol. TEA is an organic amine mixed corrosion inhibitor where adsorption to the surface of the metal is considered to be the main inhibitive effect [10, 11]. Once the TEA has adsorbed to the surface it forms a protective film that will continue to protect the substrate from water and aggressive ions reaching the surface. The use of TEA filled microcapsules can provide an autonomous healing effect for the coating. Released TEA can form a protective layer in the areas of the coating where damaged has occurred either mechanically or water has diffused through the coating to the substrate. The release of TEA from the microcapsule is due diffusion of TEA from the core of the microcapsule through microchannels in the polymeric shell formed by osmotic swelling due to the pH change in the environment [18]. This pH change can either be from the environment around the microcapsule or from the corrosion process occurring on the exposed substrate.

The use of ECR as a low cost and low maintenance form of corrosion protection of reinforced structures has shown a positive effect on the extension of the service life. But due to the mishandling of the ECR or from the deterioration of the coating from water uptake or chloride contamination severe corrosion can occur on the reinforcing steel. In this work we characterize the corrosion inhibition effect from the addition of microcapsules filled with TEA added into the epoxy coating matrix. These microcapsules will release corrosion inhibitors when damage has occurred mechanically or from the corrosion process on exposed rebar. Figure 4 depicts a graph of the damage to a concrete structure with time for a rebar that is protected with an epoxy coating that has TEA filled microcapsules added into the epoxy matrix. Where t_{i1} is the time taken for the breakdown of the coating either mechanically or chemically. This t_{i1} is typically a larger value than the time to the initiation of corrosion for uncoated rebar. t_p is the

time taken for the migration of a high enough concentration of TEA to the exposed substrate for a complete coverage to stop the corrosion process from occurring. After protection of the exposed substrate has occurred, there will be another time taken for the initiation of corrosion to occur in the area of damaged coating which is shown as t_{i2} in Figure 4. The damage evolution of the reinforced structure after breakdown of the protective layer formed by TEA is the same as that of an uncoated rebar shown in Figure 1. Where t_c is the time that cracking is noticed on the surface of the reinforced structure, and t_s is the time that spalling of the concrete occurs. The use of epoxy coated rebar with TEA filled microcapsules will extend the service life by two main methods. The first is delaying the time taken for corrosion to become initiated on the rebar from the barrier properties of the epoxy coating, and second is when the corrosion process occurs there will be a lowering of pH in the area of damaged coating and TEA will be released from the microcapsules in the coating. Once the released TEA is at a high enough concentration to form a complete layer on the exposed substrate it will continue to protect the exposed substrate until this layer is broken down by water and aggressive ions from the environment. Comparison of an unprotected rebar with ECR with microcapsules is shown in Figure 3.

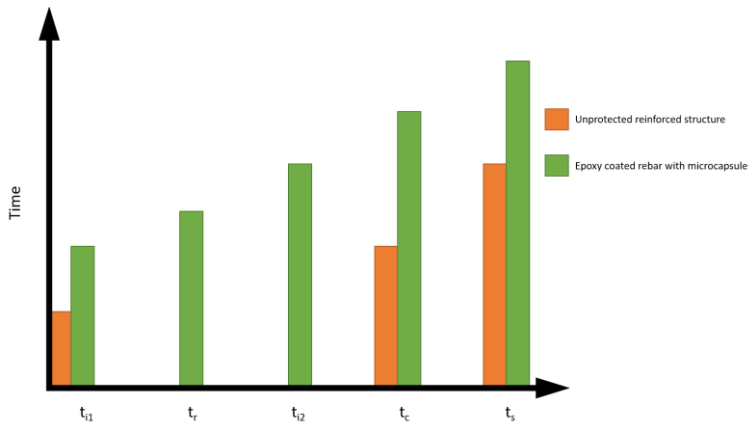

Figure 3: Comparison of unprotected reinforced structures and ECR with TEA microcapsules

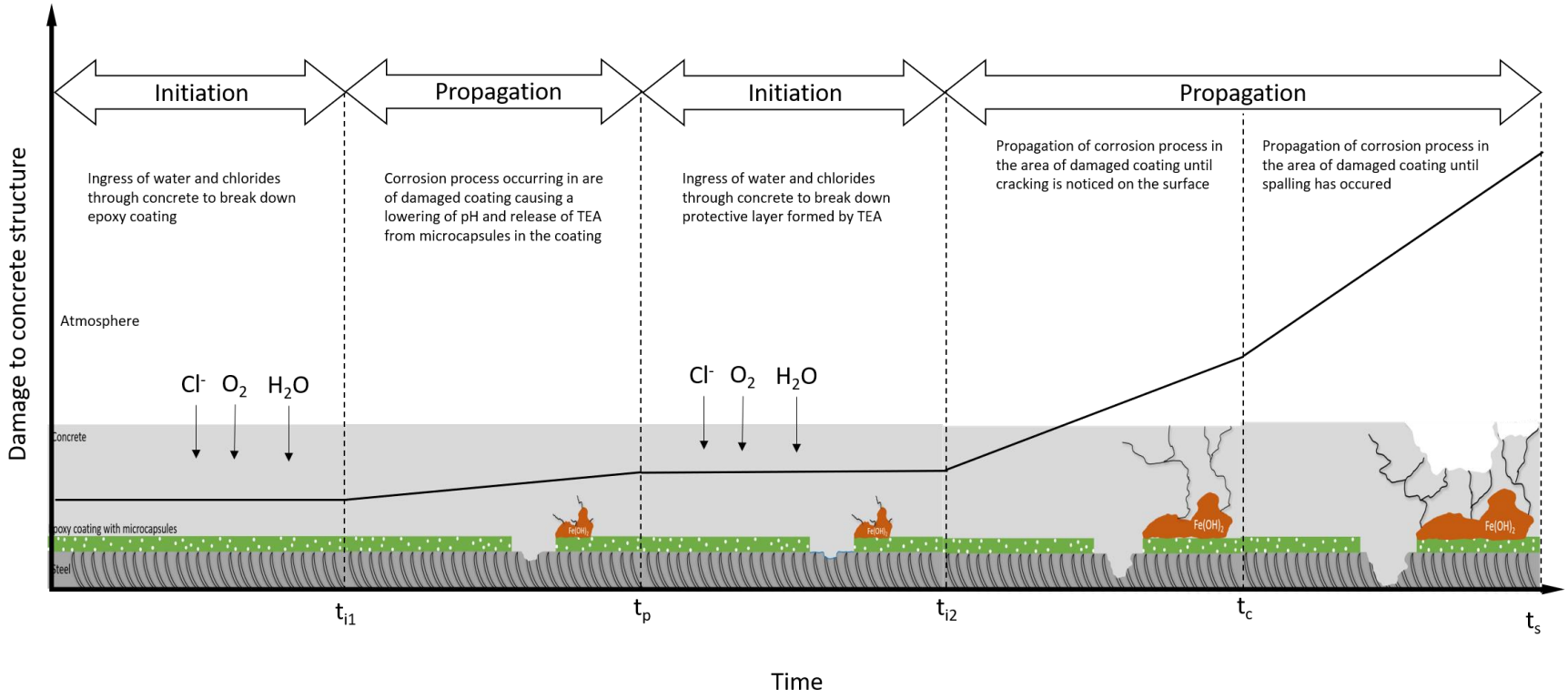

Figure 4: Service life of reinforced structure with ECR containing TEA filled microcapsules in epoxy coating matrix

2. METHODOLOGY

2.1. Encapsulation of TEA

Encapsulated of TEA was adapted from Choi et al. [18]. The microcapsules used in this study were produced at Louisiana State University. For the encapsulation, free-radical polymerization microemulsion was chosen for the encapsulation of TEA, and it involved a four-step process [19]:

1) Production of seed latex material
2) Formation of first amphiphilic shell
3) Formation of the second hydrophobic polystyrene shell
4) Charging of the capsules with TEA

The chemical used for the formation of the seed latex are: Methyl methacrylate (MMA), methacrylic acid (MAA), butyl acrylate (BA), and ethylene glycol dimethyl acrylate (EGDMA). The TEA microcapsules have two concentric shells that surround the TEA core. The charging of the TEA was driven by the neutralization of the acidic core, and the chemistry of the seed latex was chosen to ionizable in an alkaline environment.

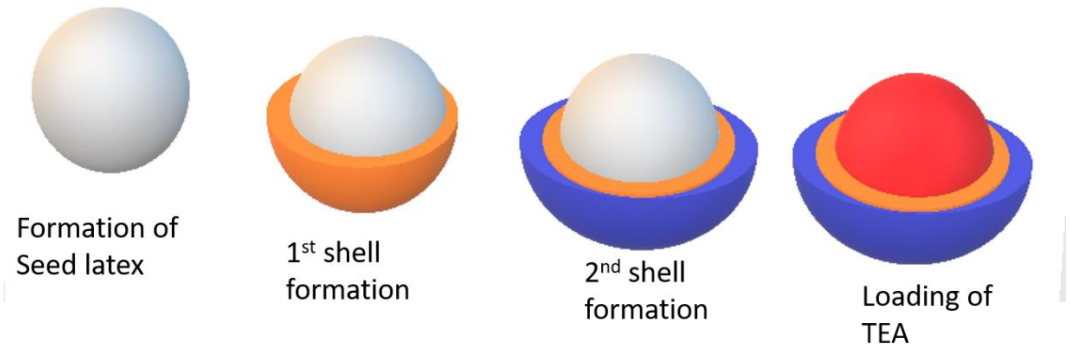

Figure 5: Formation of TEA filled microcapsules

2.2. Preparation of Test Samples

Table 1: Matrix of samples

Sample ID	TEAC Concentration (wt% of coating)	Coated	Mechanical Testing	Fog Chamber Testing	Electrochemical Testing	SVET Testing
Ctrl NC	0	N	3	3	3	0
Ctrl CD	0	Y	3	3	3	3
C10	10	Y	3	3	3	0
C30	30	Y	3	3	3	3

The epoxy coatings will be prepared with 3M Scotchkote Liquid Epoxy Coating 323 and varying concentrations of microcapsules admixed into epoxy during the mixing phase before application. To prepare the coatings to a uniform thickness the rebar to be coated will be dipped and allowed to cure hanging up in the same direction that they were dipped in. To accelerate the testing and to characterize the self-healing properties of the coating a holiday will be induced into the coating. Two scratches will be introduced into the coating with a razor blade after the coating has begun to cure. The scratches were done to simulate mechanical damage and to accelerate the corrosion process to characterize the corrosion inhibition effect of admixed microcapsule. Before testing the scratches in the coating will be inspected under low magnification to ensure that the substrate is completely exposed.

For mechanical testing low carbon steel panels will be used. The steel panels will be sandblasted and degreased before the coating is applied, and to apply the coating a bar method will be used to provide a uniform thickness in the coating. After the coating has cured the coating is scratched to expose the substrate for adhesion by tape test. The length of each scratch is roughly 1.5” and the angle where the two scratches meet is between 30° and 45°. For pull-off strength testing a 20 mm aluminum dolly is attached to the coating surface with a two-part

epoxy. Before attaching the dolly, the surface and dolly are lightly abraded to provide better adhesion between the dolly and coating. The dolly is then pressed down and held in place with tape. Excess epoxy is cleaned before being allowed to cure. The samples used for adhesion testing are shown in Figure 6.

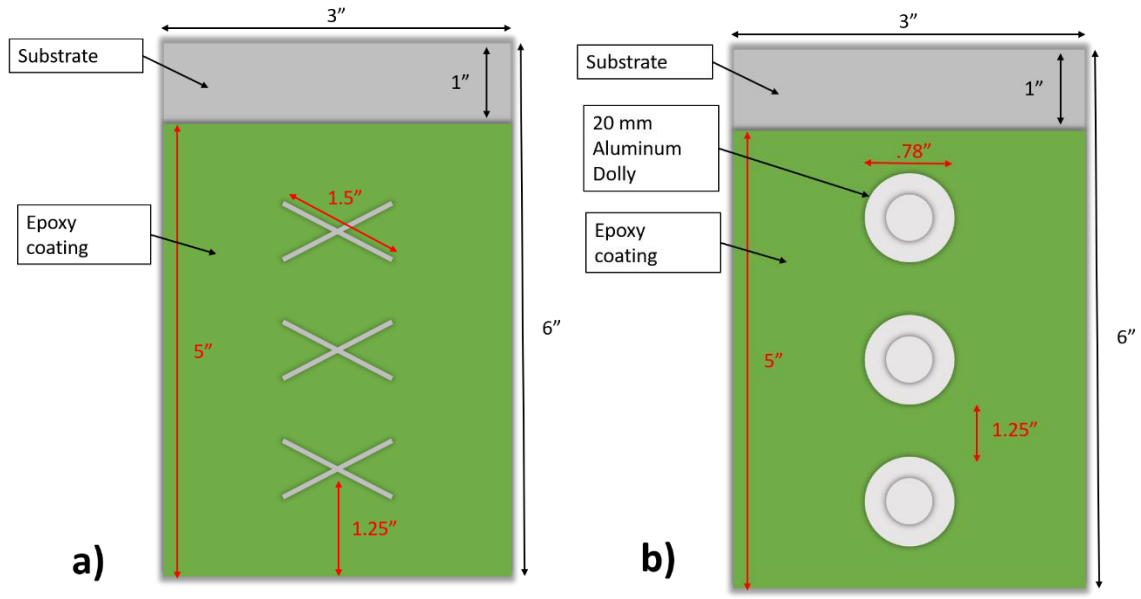

Figure 6: Adhesion testing of epoxy coating a) scratch testing, b) pull off strength testing

Electrochemical tests and fog chamber test will use the same sample geometry shown in Figure 7. The rebar used for testing are number #3 carbon steel rebar cut to 3” lengths and limited to 2.5” of exposure area. To seal off .5” of the rebar from exposure to the environment they will be mounted in a clear epoxy mount. For the samples prepared for electrochemical testing a wire will be attached to the sample before mounting for electrical connection. The average coating thickness for the samples used for fog chamber and global electrochemical testing was around 600 to 900 µm.

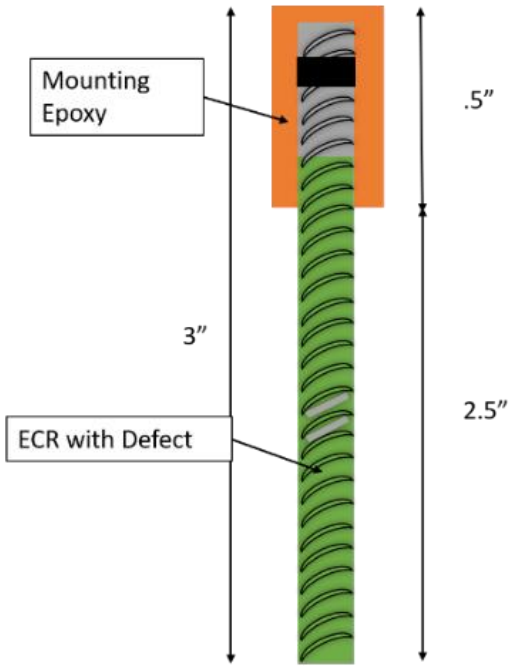

Figure 7: Test sample for fog chamber and electrochemical measurements

Figure 8 shows the sample geometry for scanning vibrating electrode testing (SVET). This a microscale non-destructive electrochemical test that measure the currents on the surface of the substrate immersed in a solution. To prepare these samples small segments of rebar will be cut and ground flat on one side and the mounted in clear epoxy so the exposed area would be the cross section of the rebar. After the mounting has cured a coating would be applied to cross section. A small scratch will be introduced into the coating using a razor blade to expose the substrate. Once the coating has cured, the specimens were ground with 320 and 1800 grit polishing pad to produce a coating thickness of 20-40 µm. The scratch was used to expose the substrate so the corrosion inhibition effect can be investigated for the samples with the addition of microcapsules.

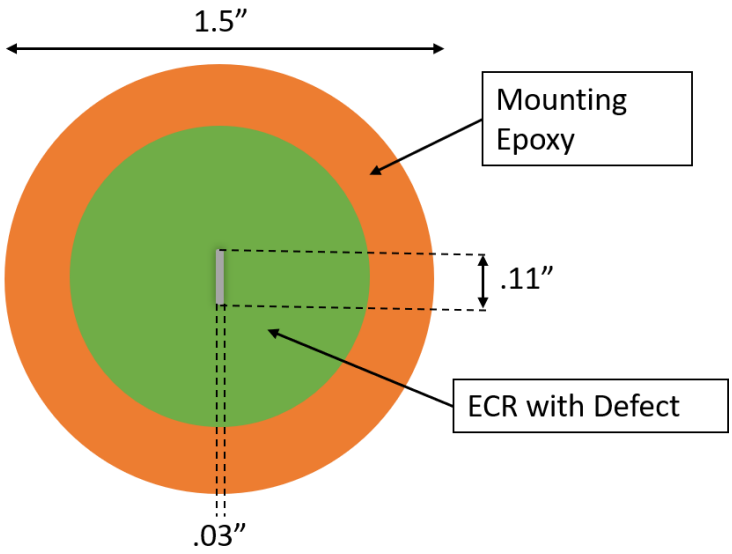

Figure 8*:* Test sample for SVET measurements

2.3. Mechanical Testing

The addition of admixtures into epoxy coatings can have an effect on the adhesion of the coatings to the substrate. The effect of the addition of microcapsules on the adhesion of the coating to the substrate will be tested following ASTM D3359: Standard Test Method for Measuring Adhesion by Tape Test [20], ASTM D2197: Adhesion of Organic Coatings by Scrape Adhesion [21], and ASTM D4541: Pull-off Strength of Coatings Using Portable Adhesion Testers [22]. For ASTM D3359 testing pressure sensitive tape was placed on the cut on the coating in line with the smaller angle formed by the two cuts. The tape was pushed down by hand first, then a blunt object was used to smooth out the rest of the tape, except to leave a small area free on one side to be used to pull. After the tape had been smoothed, it was allowed to rest for one minute. Using the free end of the tape, it was pulled off quickly as close to 180° as possible. The tested area is inspected for any coating that has come off of the substrate during testing. From ASTM D3359 there is a qualitative ranking for the performance of the coatings

[20]: 5A no peeling or removal. 4A trace peeling or removal along incisions or at their intersection, 3A jagged removal along incisions up to 1/16” on either side, 2A jagged removal along most of the incisions up to 1/8” on either side, 1A removal from most of the area of the cut under the tape, 0A removal beyond the area of the cut. ASTM D4541 pull-off strength testing was performed with a self-aligning tester and 20mm aluminum dollies attached to the surface with a two-part epoxy. The dollies were pulled at a rate of 30 psi/s. The different coatings were compared in the amount of force required to remove the dolly. The mode of failure was also compared for the coatings whether it was an adhesion failure at the dolly/coating interface or coating/substrate interface, or a cohesive failure in the coating. For scrape testing per ASTM D2197 the adhesion of the coated was tested by moving the coated panels under a metal loop that was weighted down with increasing weight. The weight was increased up to a maximum of 10 kg. Between each test the coating was inspected for coating removal. The three methods were used to qualitatively and quantitively characterize the adhesion of the coating to the substrate.

2.4. Global Electrochemical Testing

Open Circuit potential (OCP), linear polarization resistance (LPR), and electrochemical impedance spectroscopy (EIS) are used to characterize the corrosion resistance of the immersed samples in a simulated concrete pore solution. Potentiodynamic polarization testing was done to determine the testing solution for EIS, OCP, and LPR. All tests will use a three-electrode system and with a Gamry 1000 interface potentiostat. The three-electrode system will consist of a saturated calomel electrode (SCE) as the reference electrode (RE), graphite rod as the counter electrode (CE), and the prepared rebar sample as the working electrode (WE). The samples will be immersed for 3 days with electrochemical measurements taken periodically throughout the exposure time. OCP is a measure of the open circuit potential (corrosion potential) of the WE

with respect to a RE. During immersion, OCP was measured for the first 12 hours and 1 hour before each LPR and EIS test run. This value is a steady state concept that can describe the surface conditions between the rebar/electrolyte interface depending on the pH of the environment. Before LPR, EIS, and polarization the OCP was recorded until small perturbation was reached (or dynamic steady state). LPR is a non-destructive DC technique that can measure the kinetics of the system. This technique polarizes the WE by a small amount (20 mV) in the anodic and cathodic direction, and the current is recorded. The scan rate for LPR testing was 0.125 mV/s. EIS is a non-destructive alternating current (AC) technique were small amplitude sinusoidal waves between the counter and the working electrode and the current response is recorded. The EIS spectra was measured in the frequency range of 100 kHz to 10 mHz, with a small perturbation signal of 10 mV vs OCP. The set up for electrochemical testing is shown in Figure 9.

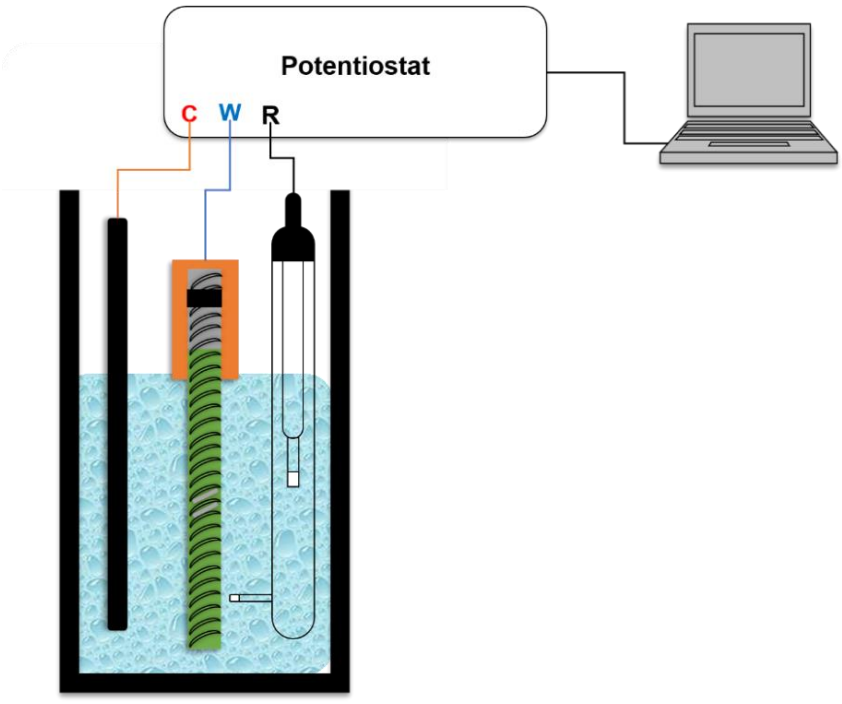

Figure 9*:* Electrochemical Testing for Immersion of Rebar

The environment for electrochemical testing was chosen to simulate the conditions that the rebar will be subject to during its service life. To determine the testing environment for further electrochemical testing, polarization tests were run in two simulated pore solutions. The first solution was a saturated calcium hydroxide ($Ca(OH)_2$) solution which is a typical solution that has been used to simulate aged non-carbonated concrete in other studies [23-27]. The second solution was chosen to simulate an aged, carbonated concrete with chloride ingress [28]. Chemical composition of two solutions is shown in Table 2.

Table 2: Chemical composition of polarization solutions

Solution	Label	$Ca(OH)_2$	$NaHCO_3$	Na_2CO_3	NaCl
Aged noncarbonated concrete	SC	4 (g/L)	0	0	0
Aged carbonated concrete	CSPS	0	1.26 (g/L)	.529 (g/L)	35 (g/L)

2.5. Fog Chamber Exposure

Testing in the fog chamber will use a 5% by weight NaCl fog and at a temperature of 35°C. The samples will be exposed for 7 days. Visual inspection of the samples was performed every hour for the first six hours of exposure, and then once a day for the rest of the exposure time. The usefulness of the fog chamber is that samples be exposed to extremely harsh conditions that expedite the corrosion process. This allows for a quick and effect qualitative comparison of corrosion inhibition properties of the admixed microcapsules. Figure 10 shows the fog chamber used for exposure, and how the samples are arranged in the fog chamber during exposure.

Figure 10: Fog Chamber and set up inside fog chamber

2.6. SVET

Scanning vibrating electrode technique (SVET) is a non-destructive localized electrochemical testing technique. SVET is a measurement of the local voltage drops in a solution between the wire of the SVET probe and the surface. This voltage drop is due to the local currents on the surface from the corrosion process occurring. Testing was done at open circuit potential and the testing solution was carbonated simulated pore solution with a solution resistance of 1.70 ohm-cm. The scanning probe was set to a height of 75 µm above the coating. The scanning area was 1500 by 150 µm making sure to capture the damaged area of the coating along with part of the intact coating. Scan rate for the X and Y direction were 5 µm/s. Figure 11 shows the set up for SVET testing. For SVET measurements a VersaSCAN system with a SVET probe was used.

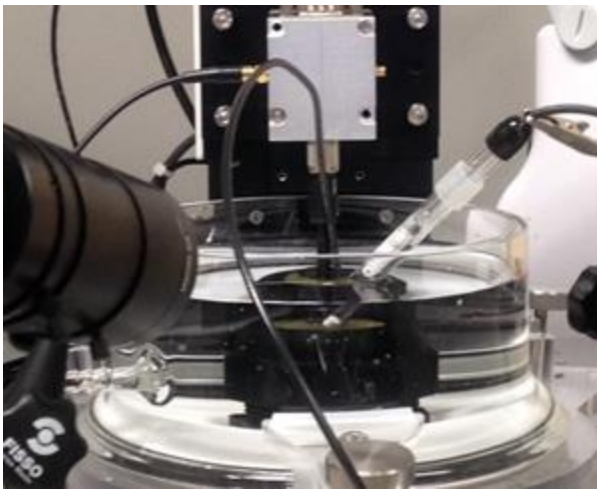

Figure 11: SVET Testing Setup

2.7 SEM/EDS

For further characterization of the corrosion inhibitive effect the addition of microcapsules has on the epoxy coating, the exposed substrate was observed with scanning electron microscope (SEM) and energy dispersive x-ray spectroscopy (EDS). Before observation the samples were exposed for 24 hours in the carbonated simulated pore solution. A JCM-6000PLUS Neoscope Benchtop SEM was used for SEM/EDS measurements with a voltage of 15 kV.

3. RESULTS AND DISCUSSION

3.1. Mechanical Testing

The results from the mechanical testing of the epoxy coating with and without microcapsule are shown in Figures 12-14. Testing was performed in the dry condition and at room temperature. Every coating was tested 3 times on the same substrate with an average coating thickness of around 500 µm. The variability between the tests on the same coating could be due to the human error from cutting the coating to expose the substrate, application of epoxy to attach dolly, or the pull rate of scrape testing. From ASTM D2197 all three coatings had little to no damage at the maximum weight allowed from the standard. Figure 12 shows the results from scrape testing. Ctrl CD only showed a small indentation on the surface, and coatings C10 and C30 had small areas of coating loss along the scrape. Using the qualitative ranking from ASTM D3359 each test was ranked and compared. The rankings of each test are shown in Table 3. Ctrl CD showed the least amount of coating loss, and C10 showed the highest amount of coating loss. Table 4 shows the pull off strength values from ASTM D4541 testing. All pull off strength values were very close to each other, this could be due to the failure from pull off strength testing was mainly due to the adhesion of the dolly to the coating. From Figure 14 it can be seen that Ctrl CD showed the least amount of coating loss from pull off testing, and C30 show the most coating loss in the three tests. The addition of microcapsules showed a decrease in the adhesion strength of the coating, which be seen by more coating being removed in all three tests. The decrease in the adhesion strength of the coating could be due to the increased viscosity of the coating with the addition of microcapsules [29]. When the microcapsules were admixed into the epoxy resin during mixing the viscosity of the resin was increased, which in turn increased

the viscosity of the epoxy coating. With the increase in viscosity there is less time for the for the coating to mechanically adhere to the surface which would lower its adhesion strength.

Table 3: Results of tape adhesion testing

Sample	Test 1	Test 2	Test 3
Ctrl CD	4a	3a	3a
C10	4a	1a	2a
C30	3a	4a	2a

Table 4: Pull of strength measured from ASTM D4541 Testing

Sample	Test 1 (psi)	Test 2 (psi)	Test 3 (psi)	Average (psi)
Ctrl CD	182	202	314	232.67
C10	208	235	246	229.67
C30	178	236	324	246

Figure 12: After pictures of ASTM D2197 a) Ctrl CD b) C10 and c) C30

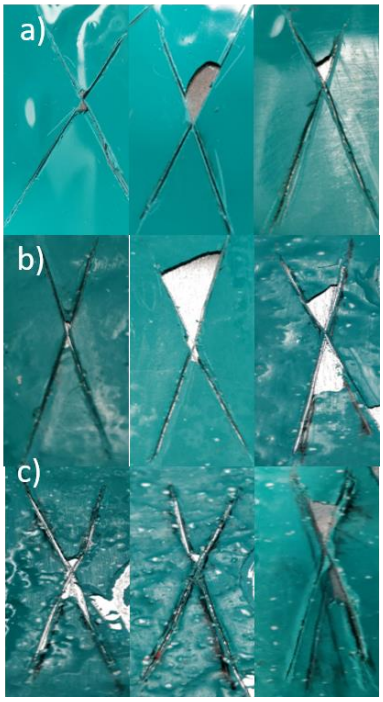

Figure 13: After pictures of ASTM D3359 testing a) Ctrl CD, b) C10, and c) C30

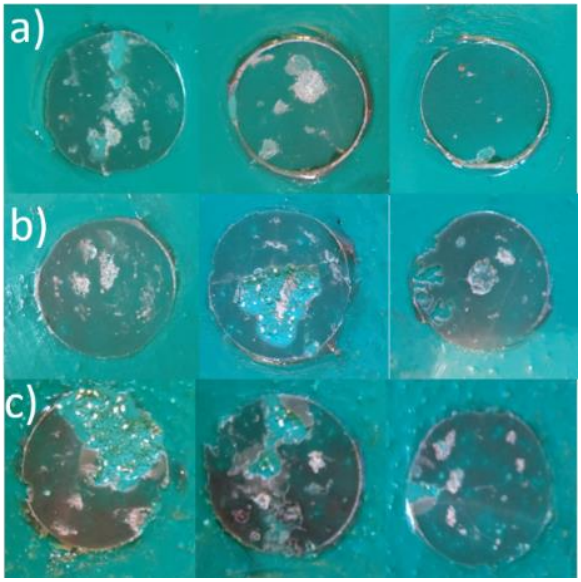

Figure 14: After pictures of ASTM D4541 testing a) Ctrl CD, b) C10, c) C30

3.2. Global Electrochemical Testing

3.2.1 Potentiodynamic Polarization

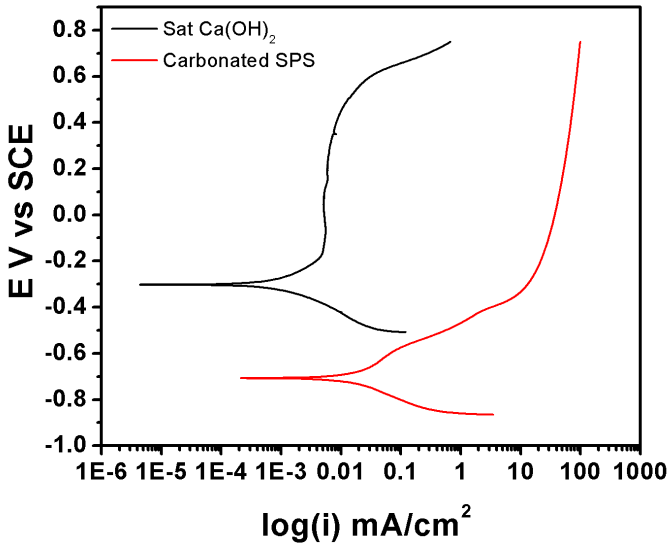

Figure 15: Polarization of rebar in saturated calcium hydroxide and carbonated simulated pore solution

Results from the polarization testing are shown in Figure 15 and Table 5 shows the OCP, i_{corr}, β_a, and β_c calculated from polarization curve. It can be seen that the corrosion current density for the rebar immersed in SC solution is an order of magnitude lower than for the rebar in CSPS.

Table 5: Polarization testing in two different simulated pore solutions

Solution	OCP (mV)	icorr (mA/cm^2)	β_a (mV)	β_c (mV)
Saturated Ca(OH)$_2$	-302.5	.001490	243.2	143.1
Carbonated simulated pore solution	-707.8	.014211	140.2	99.6

From the OCP value in the SC and CSPS solution and pH of the environments passivity is expected to be seen [30]. The sample immersed in the SC solution showed a passive layer forming around -200 mV vs SCE, and extending to a breakdown potential of around 600 mV vs SCE giving a passive window range of 800 mV, with a passive current of around .0055 mA/cm^2. The rebar immersed in CSPS shows very a quick activation and continued to stay active until a limiting current of around 50 mA/cm^2. From the polarization curve it can be seen that a passive film was not formed on the rebar during testing in CSPS. The passive layer that would typically be formed by $Fe(OH)_2$ in an alkaline aqueous environments is attacked by bicarbonate (HCO_3^-) to form $Fe(CO_3)$, which can then form the complex anion of $Fe(CO_3)_2^{2-}$ [31]. Due to this behavior of iron in bicarbonate/carbonate solutions, CSPS was chosen to use in further electrochemical testing since rebar exposed to this environment will freely corrode. This is useful for determining the self-healing and inhibiting effect of the microcapsules, since the lower pH of the solution and the corrosion reaction will allow the release of the corrosion inhibitor [18].

3.2.2 Open Circuit potential

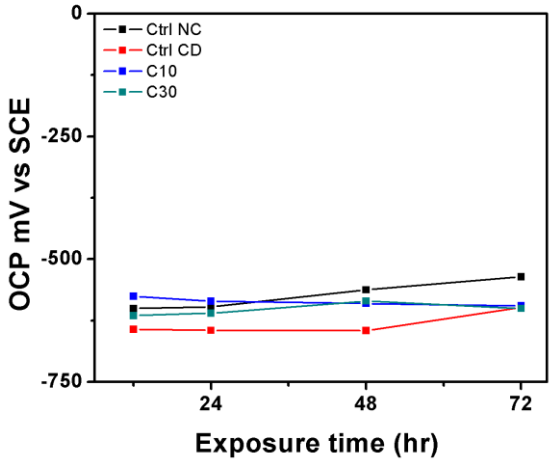

Figure 16: OCP values of immersed samples for 3 days exposure in carbonated simulated pore solution

Figure 16 shows the OCP values for the immersed samples. The OCP values for all samples stayed relatively stable for the duration of testing. At the beginning of immersion C10 showed the most positive OCP value at -575 mV vs SCE, and at the end of testing Ctrl NC showed the most positive OCP at-535 mV vs SCE. Ctrl CD showed the most negative OCP values for the duration of testing. All the OCP values for the samples fall into a range of -535 mV vs SCE to -645 mV vs SCE. The difference between the OCP values measured at each exposure time is not large enough to determine if different processes are occurring on the surface. From ASTM C876 if the OCP of the rebar in concrete is below -350 mV vs CSE (-395 mV vs SCE) there is a greater than 90% chance that corrosion is occurring on the rebar [32]. The more positive value of OCP that would be expected from the formation of a TEA protective film is not seen, and this could be due to the limitation of the way that the OCP is measure. The formation of a TEA layer is most likely formed fist at the edges of the damaged coating since this were the microcapsules are located.

3.2.3 Linear Polarization Resistance

Figure 17 the polarization resistance (Rp) and corrosion rate (CR) calculated is shown. The polarization resistance can be measured by determining the slope of the current vs potential line around OCP [33]:

$$Rp = \left(\frac{\Delta E}{\Delta I}\right)_{\eta \to 0} \quad (3)$$

Where η is the over potential ($E_{applied} - E_{corr}$), $\Delta E$is the change in potential, and ΔI, is the change in current. The corrosion rate is calculated from the corrosion current density which is calculated from the Rp obtain from polarization resistance.

$$i_{corr} = \frac{B}{Rp*A} = \frac{\beta_a*\beta_c}{2.3*(\beta_a+\beta_c)*Rp*A} \quad (4)$$

Where β_a an β_c are the anodic and cathodic Tafel slopes, which were calculated from the polarization curves, and A is the exposed area of the rebar including damaged area and intact coating. The corrosion rate is a calculation of the uniform corrosion in units of distance per time.

$$CR = \frac{k*EW*i_{corr}}{d} \quad (5)$$

Where k is a constant that depends on the chosen units of CR, EW is the equivalent weight of the material, i_{corr} is the corrosion current density, and d is the density of the material. The material used in this study is carbon steel rebar, with an equivalent weight of 27.92 and a density of 7.87 g/cm^3 [34]. It can be seen that the Rp of the samples with damaged coating are roughly 100 times larger than non-coated sample. This is due to most of the sample being protected by the coating and only a small exposed area due to the damage in the coating. All samples had a slight decrease in the Rp with increase in exposure time. C30 had the highest Rp for the entirety of testing, and Ctrl CD had the lowest Rp out of the coated samples.

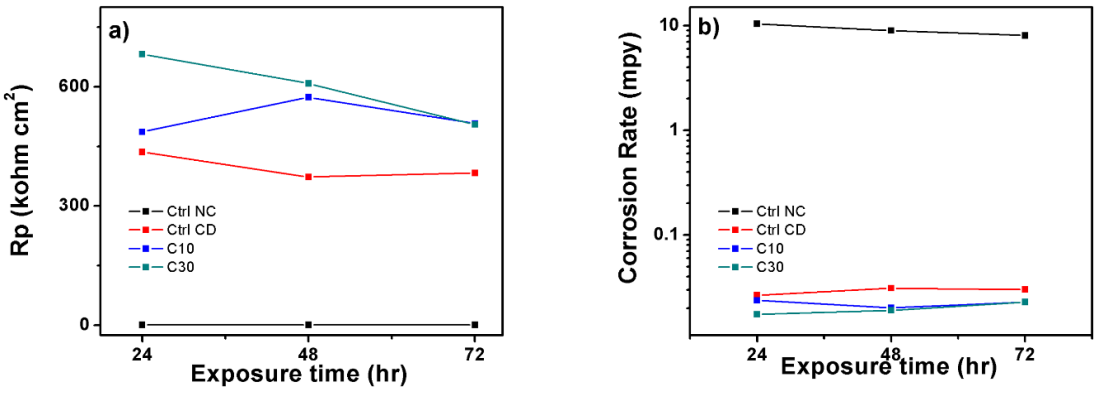

Figure 17: (a) Polarization resistance values from LPR, (b) corrosion rates calculated from Rp, (c) Zoomed portion of corrosion rates of Ctrl CD, C10, and C30 in carbonated simulated pore solution

The polarization resistance is the resistance of a charge to cross the electric double layer at the metal/solution interface [33]. The higher the polarization resistance the better the corrosion resistance. This increase in polarization resistance of C10 and C30 compared to control samples could be due to the formation of a TEA layer on the exposed area. Which, would limit the penetration of water and aggressive species such that further corrosion process is inhibited.

3.2.4 Electrochemical Impedance Spectroscopy

The complex impedance response of the samples allows for the evaluation of different components of the system such as the protective layers, polarization resistance and double layer capacitance [35]. Different frequency regimes of the EIS spectra correspond to the different components of the system. The most common frequency regime used for corrosion performance comparison between different systems is the low frequency impedance response. This is due to the fact that the low frequency response can be correlated to the corrosion process at the metal/electrolyte interface. The fitting of a theoretical equivalent circuit composed of real circuit elements can be used to evaluate the physical components of the system. Figures 18 through 21 show the circuits used to fit the EIS response of all samples.

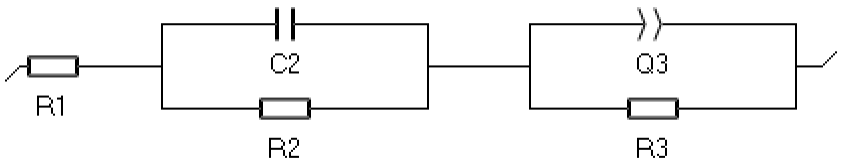

Figure 18: 1st day exposure of Ctrl NC

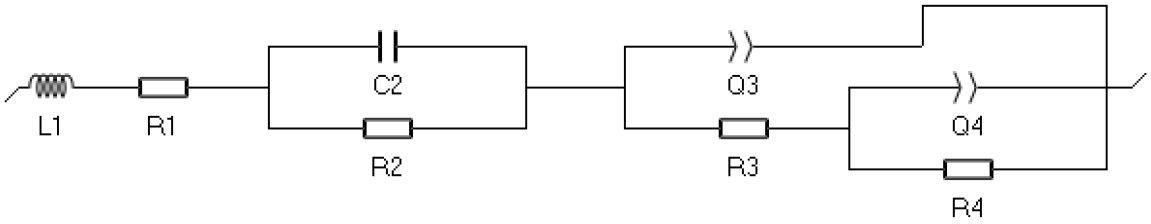

Figure 19: 2nd day exposure of Ctrl NC

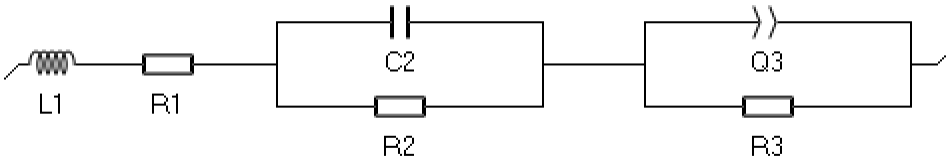

Figure 20: 3rd day exposure of Ctrl NC

Figures 18 through 20 are the circuits used to fit the EIS data from Ctrl NC samples. A RC or LRC circuit was added to have a better fit in the high frequency regime for all days of exposure. Capacitive and inductive loops that are seen in the high frequency could possibly be due to a large reference electrode impedance due to the voltage divider effect [36]. The circuit elements that are used to create a better fit in the high frequency regime have little importance to the other circuit elements that simulate physical properties. Figures 18 and 20 are a commonly used Randles circuit with the addition of a constant phase elements (CPE) to simulate the double layer capacitance (Cdl) since the phase angle is not -90°. For the second day there was the addition of second time constant in the middle to high frequency so a second time constant was added to the circuit for a better fitting. Table 6 and 7 show the definitions of the circuit elements in Figures 18-20.

Table 6: Circuit elements for fitting of Ctrl NC EIS response 1st and 3rd day

Circuit element	Definition
R1	Solution resistance (Rs)
L1	High frequency inductance (L_{HF})
R2	High frequency resistance (R_{HF})
C2	High frequency capacitance (C_{HF})
R3	Polarization resistance (Rp)
Q3	Double layer capacitance (Cdl)

Table 7: Circuit elements for fitting of Ctrl NC EIS response 2nd day

Circuit element	**Definition**
R1	Solution resistance (Rs)
L1	High Frequency inductance (L_{HF})
R2	High frequency resistance (R_{HF})
C2	High frequency capacitance (C_{HF})
Q3	Capacitance of the corrosion products (CC)
R3	Pore resistance of corrosion products (RC)
Q4	Double layer capacitance (Cdl)
R4	Polarization resistance (Rp)

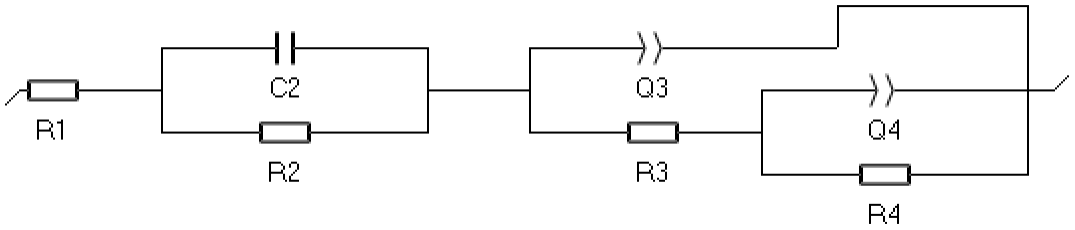

Figure 21: Equivalent circuit for samples Ctrl CD, C10, and C30

Figure 21 show the equivalent circuit used for the fittings of the samples with a coating. Similar to the circuit in Figure 16 there is a RC circuit in series with the rest of the circuit for better fitting in the high frequency regime. The circuit without the high frequency RC element is commonly used to fit coated metals [37]. Table 8 shows the definitions of the equivalent circuit elements in Figure 21. The use of CPEs (Q3 and Q4) rather than pure capacitors was due the phase angles of these capacitances not being -90°. The polarization resistance calculated from EIS is the same polarization resistance calculated from LPR. Double layer capacitance is the capacitance of the electrical double layer that is formed at the metal/solution interface. CC and RC are properties of the coating, where CC is the capacitance of the intact coating and RC is the resistance of the connected pores of the coating. As immersion time increases these values are expected to lower due to the water intake into the coating.

Table 8: Circuit elements for fitting of coated samples EIS response

Circuit element	Definition
R1	Solution resistance (Rs)
R2	High frequency resistance (R_{HF})
C2	High frequency capacitance (C_{HF})

Table 8 Continued: Circuit elements for fitting of coated samples EIS response

Q3	Capacitance of the coating (CC)
R3	Pore resistance (RC)
Q4	Double layer capacitance (Cdl)
R4	Polarization resistance (Rp)

Figures 22 and 24-26 show the Nyquist, bode, and phase angle representation of EIS for all samples. The Nyquist show the processes that are occurring in the system. Bode plot shows the quantitative magnitude of the impedance values, while phase angle representation shows what kind of circuit elements are formed in the system. From the Nyquist and phase angle of Ctrl NC it can be seen that on the first and third day of immersion there are two-time constants present, which are attributed to the high frequency capacitive or inductive loops due to the high impedance of the reference electrode [36] and low frequency response of the faradaic processes occurring on the rebar. On the second day of immersion there was addition of new time constant in the middle frequency (10-10,000 Hz), this could be due to the corrosion products forming on the surface of the rebar. The Nyquist and phase angle representations of the coated samples showed that there are three-time constants. The high (>10 kHz) and low frequency (<10 Hz) response are from the same sources as those for Ctrl NC, but the middle to high frequency response is due to the coating and if any possible films have formed on the exposed surface. Ctrl NC showed the lowest impedance out of all the samples due to it being uncoated metal. It can also be seen that the metal did not show any capacitive behavior until frequencies below 10 Hz, which in this frequency regime is due to the capacitance of the electrical double layer. Except on the second day there was capacitive behavior starting around 10 kHz which could be

due to a layer of corrosion products forming on the surface. This layer will behave similar to that of a poor-quality coating, not providing much protection due to its porosity but still has capacitive and resistive properties. All samples showed similar characteristics in the high frequency regime since they were exposed to the same testing environment and testing configuration. The samples with the addition of microcapsules showed more capacitive behavior in the high (10^4 Hz) to medium (10^0 Hz) than the control sample. This can be seen by the more negative phase angle values, and the start of the capacitive loop at higher frequencies. With the addition of TEA containing microcapsules to the coating this increase in the capacitance could be due to film that has formed on the substrate. We know that it most likely not a passive film being formed on the steel, but possibly due to a film that is formed from the TEA being released from the coating. With increasing exposure Ctrl CD and C30 both showed shifts to more resistive behavior with increasing exposure time, while C10 did not change very much. For Ctrl CD in the first day of immersion corrosion products could be formed and built up on the exposed surface, but due to the bicarbonates in the solutions the corrosion products formed would be dissolved as the complex anion $Fe(CO_3)_2^{2-}$ [31]. By the second day of immersion C10 and C30 both had very similar responses. This dissolution of the corrosion product would lower the capacitance in the middle to high frequency with immersion time.

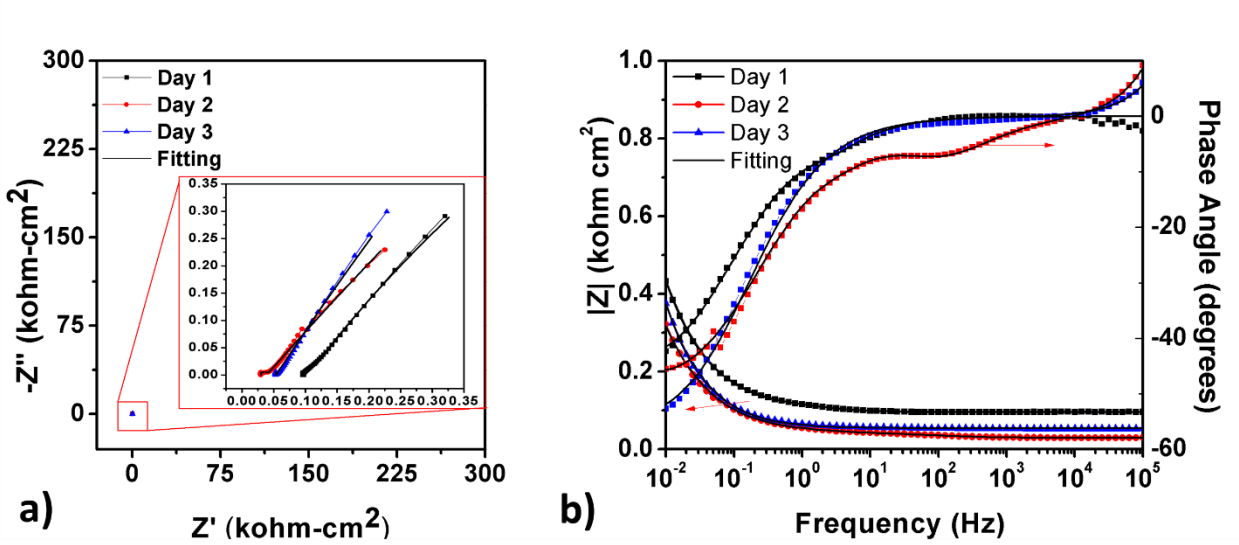

Figure 22: Nyquist, bode, and phase angle of Ctrl NC in carbonated simulated pore solution

C30 showed a similar trend of that of Ctrl CD, but it did not decrease as much and the response became very similar to that of C10. This could be due more TEA being able to react and form a more complete film on the C30 sample after mechanical damage has occurred and during the immersion process. This is possibly due similar coverage area of TEA on the exposed are. Even though C30 would have a higher concentration of microcapsules there would still be a certain time until TEA can be released to the surface due water up take in to the coating to provide a path of diffusion from the microcapsule to the exposed substrate. In the low frequency regime, the samples with the addition of microcapsules show a lower maximum phase angle value than Ctrl CD. The close the phase angle to -90° the better the corrosion resistance, but Ctrl CD showed a smaller basin of the phase angle values in the low frequency regime, this could be due to the stability of the corrosion layer that is formed on the surface of the Ctrl CD sample is not as stable as the TEA layer formed for microcapsule samples. The last point of the impedance magnitude can be used to compare the corrosion resistance of different systems, due to the value

being contributions of resistance and capacitance at that frequency. Figure 23 shows the change in the lowest frequency impedance magnitude with exposure time. Of all the coated samples C30 Showed the highest impedance magnitude in the low frequency regime, with C10 next highest which was above Ctrl CD. On the first day the phase angle for all samples were similar. Ctrl CD showed the most capacitive behavior with the highest phase angle value on the second and third day of exposure. From the phase angle we can see what process provides a larger contribution in the impedance magnitude calculation, around -45° the contribution from the capacitance and resistance is 1:1. Increasing exposure time for all samples showed a decrease in impedance magnitude at a frequency of 0.01 Hz. This lowering in impedance magnitude is possibly due to the corrosion process beginning on the exposed metal. With the lowering of the polarization resistance at the metal/electrolyte interface the impedance magnitude will decrease even with an increase in the capacitance of the double layer, which can be seen for Ctrl CD.

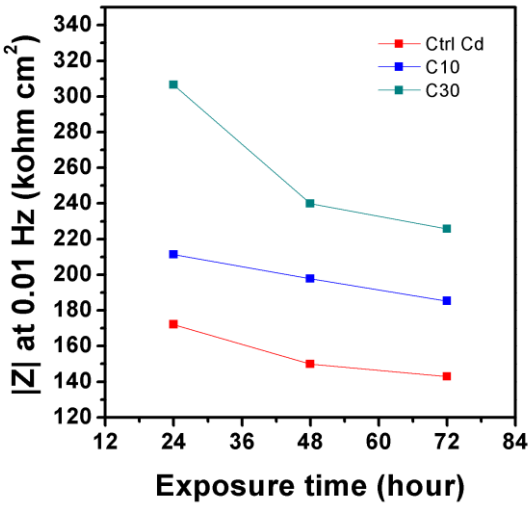

Figure 23: Impedance magnitude of coated samples at 0.01 Hz in carbonated simulated pore solution

Table 9 shows the results of the fitting of the equivalent circuits to the EIS response of the samples. The Rp determined from these fittings do not match the trends of the bode or of the Rp

calculated from LPR. Since the response of the samples are not perfect resistors and capacitors this can lead to depressed and open-ended semi-circle arcs. When this occurs fitting EIS response with an equivalent circuit can lead either to an over or under estimation of the values in question. From Table 9 it can be seen that with exposure time the high frequency response does not vary. This is partly due to the same testing configuration and equipment being used for all testing. There is some variation in the values for Rs and R_{HF} which are the solution resistance and high frequency resistance respectively. This variation could come from the fitting process dealing with open loops, but the combination of these two values does stay around the same value for the coated samples and uncoated samples. RC and CC show the properties of the coating observed in the middle to high frequency. RC for the samples without microcapsules showed a decrease with exposure time and samples with microcapsules showed an increase. This could be due to the TEA layer forming on the surface which would increase the resistance measured in this frequency regime.

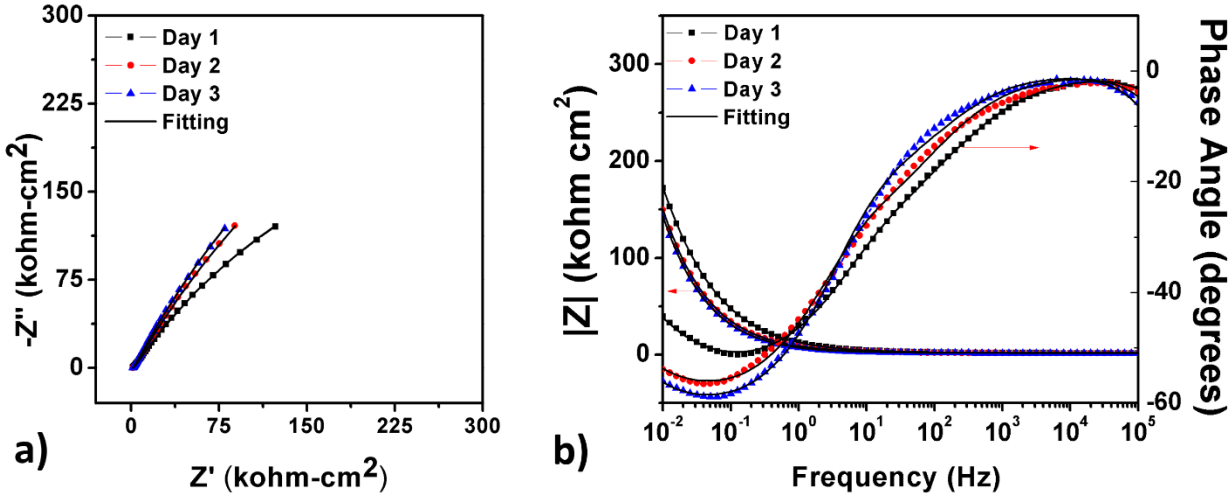

Figure 24: Nyquist, bode, and phase angle of Ctrl CD in carbonated simulated pore solution

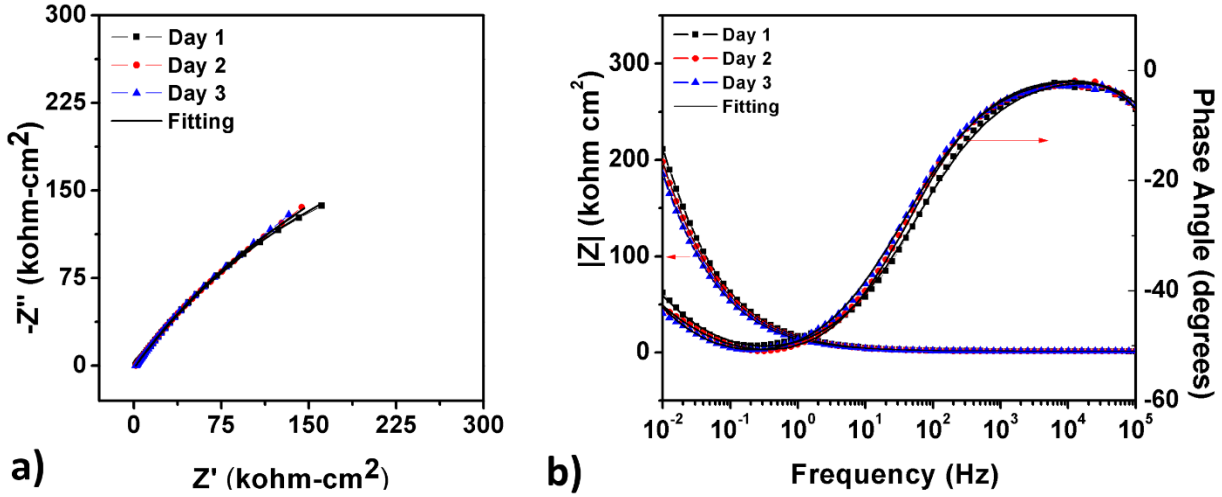

Figure 25: Nyquist, bode, and phase angle of C10 in carbonated simulated pore solution

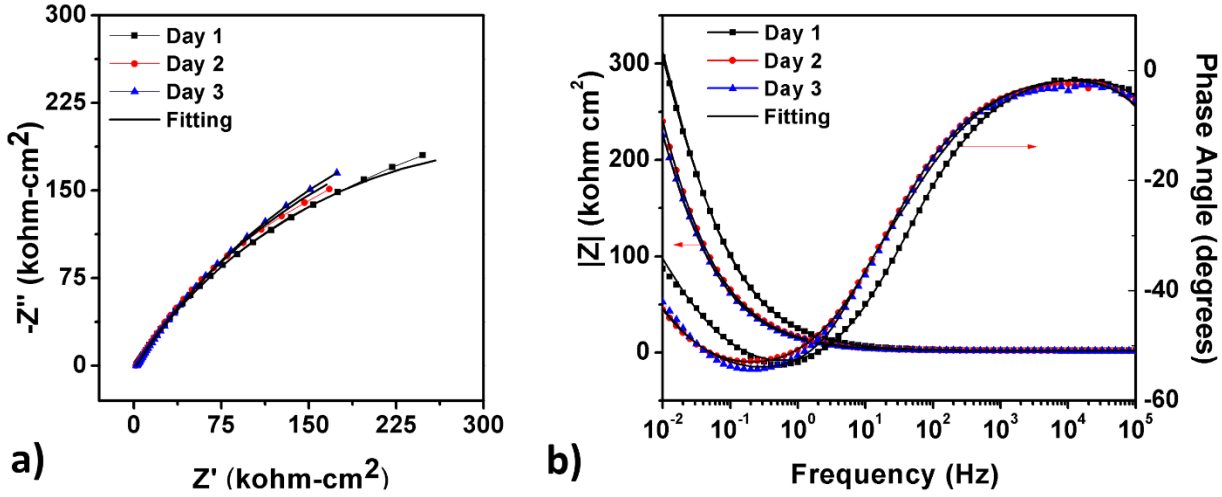

Figure 26: Nyquist, bode, and phase angle of C30 in carbonated simulated pore solution

Table 9: Equivalent circuit fitting values

Sample	L_{HF} (H)	Rs (kohm-cm^2)	R_{HF} (kohm-cm^2)	C_{HF} (F/cm^2)	CC ($Fs^{(n-1)}/cm^2$)	nC	RC (kohm-cm^2)	Cdl ($Fs^{(n-1)}/cm^2$)	ndl	Rp (kohm-cm^2)
Ctrl NC – Day 1	-	0.096	0.0081	.0071	-	-	-	0.015	0.6343	3.75
Ctrl NC – Day 2	$0.19*10^{-6}$	0.030	0.025	.0017	$7.37*10^{-4}$	0.731	0.012	0.018	0.6219	3.19
Ctrl NC – Day 3	$0.23*10^{-6}$	0.041	0.013	.00094	-	-	-	0.018	0.6750	9.34
Ctrl CD – Day 1	-	$1.88*10^{-15}$	1.641	$4.52*10^{-11}$	$1.72*10^{-5}$	0.6002	5.09	$1.08*10^{-5}$	0.6561	758.88
Ctrl CD – Day 2	-	$1.07*10^{-15}$	1.609	$7.58*10^{-11}$	$2.02*10^{-5}$	0.6498	3.94	$2.02*10^{-5}$	0.6922	1280.44
Ctrl CD – Day 3	-	$1.96*10^{-14}$	1.562	$1.09*10^{-10}$	$1.77*10^{-5}$	0.7025	1.65	$2.8*10^{-5}$	0.6917	1273.52
C10 – Day 1	-	0.0020	1.469	$1.06*10^{-10}$	$1.97*10^{-5}$	0.6056	5.70	$6.48*10^{-7}$	0.2566	864.64
C10 – Day 2	-	0.108	1.432	$1.42*10^{-10}$	$1.61*10^{-5}$	0.6685	11.12	$7.06*10^{-6}$	0.4471	1083.16
C10 – Day 3	-	$7.17*10^{-16}$	1.523	$1.22*10^{-10}$	$2.24*10^{-5}$	0.6166	2.93	$1.82*10^{-6}$	0.4896	795.06
C30 – Day 1	-	1.267	0.853	$3.73*10^{-10}$	$4.18*10^{-6}$	0.7629	1.49	$8.63*10^{-6}$	0.5823	699.14
C30 – Day 2	-	1.036	0.956	$3.83*10^{-10}$	$1.69*10^{-5}$	0.6345	4.18	$3.23*10^{-6}$	0.6731	842.41
C30 – Day 3	-	0.809	0.900	$3.82*10^{-10}$	$2.08*10^{-5}$	0.6316	21.62	$9.08*10^{-7}$	0.9941	773.51

3.3. Fog Chamber Testing

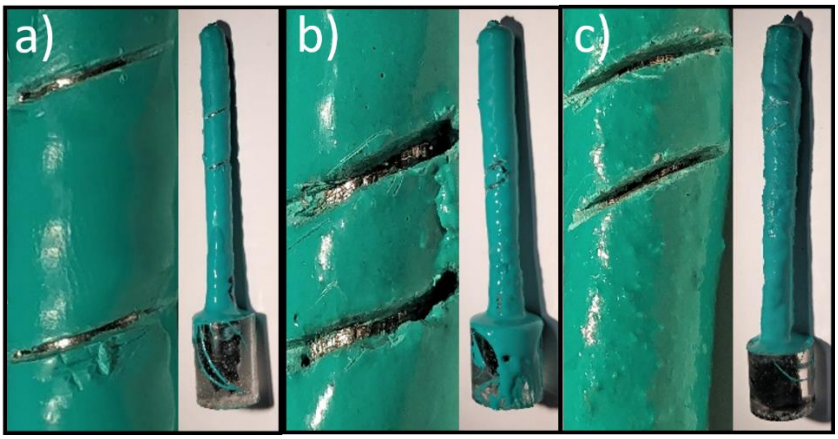

Figure 27: Initial photos of a) Ctrl CD, b) C10, and c) C30 before exposure in fog chamber

Figure 27 shows the initial condition of the ECR samples before exposure in the fog chamber. In Figures 28-30 the pictures of samples C10, C30, and Ctrl CD are shown during exposure in the fog chamber. For each sample the first 6 hours of exposure are shown along with a picture from each day of exposure. The addition of microcapsules to the epoxy showed a delay in the time it took for the exposed area to become completely corroded. Ctrl CD showed corrosion with in the first 4 hours of exposure, and by the 1st day the entire exposure area showed corrosion. C10 showed signs of corrosion by a slight discoloration of the coating due to the corrosion products by the 5th hour of exposure, but localized corrosion could be seen on the 6th hour of exposure. C30 performed similarly to C10, but did not show signs of corrosion in the first 6 hours of exposure. The exposed area of C10 was completely corroded on the 3rd day, while the exposure area of C30 was completely corroded on the 5th day. The delay in the initiation of corrosion for C10 and C30 could be due to the TEA that was released from the scratching of the coating. The scratching of the coating is to simulate mechanical damage that

can occur during the service life of the ECR. After the corrosion process has started the increase in the time it takes for C10 and C30 to have its exposed area to become fully corroded is possibly due to the release of the TEA. The TEA that would be released in this case would come from the capsules that exposed on the inside of the cut. Since the samples were not immersed in a testing solution, the release of the TEA from the microcapsules is most likely due to the corrosion process occurring in the exposed area. In the case of the samples with microcapsules the last area for the corrosion process to occur is an area nearest to the coating. This is most likely from the microcapsules that are in the edge of the coating inside the damaged area, and when the TEA is released it will protect the exposed substrate by the coating first.

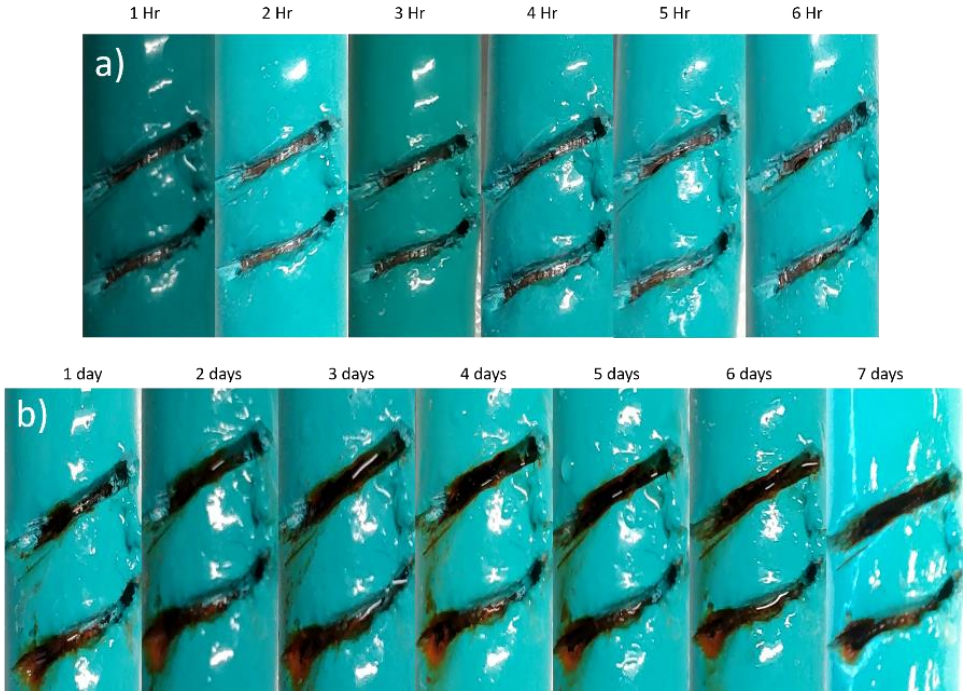

Figure 28: Exposure of C10 for a) first 6 hours of exposure, and b) 7 days inside fog chamber

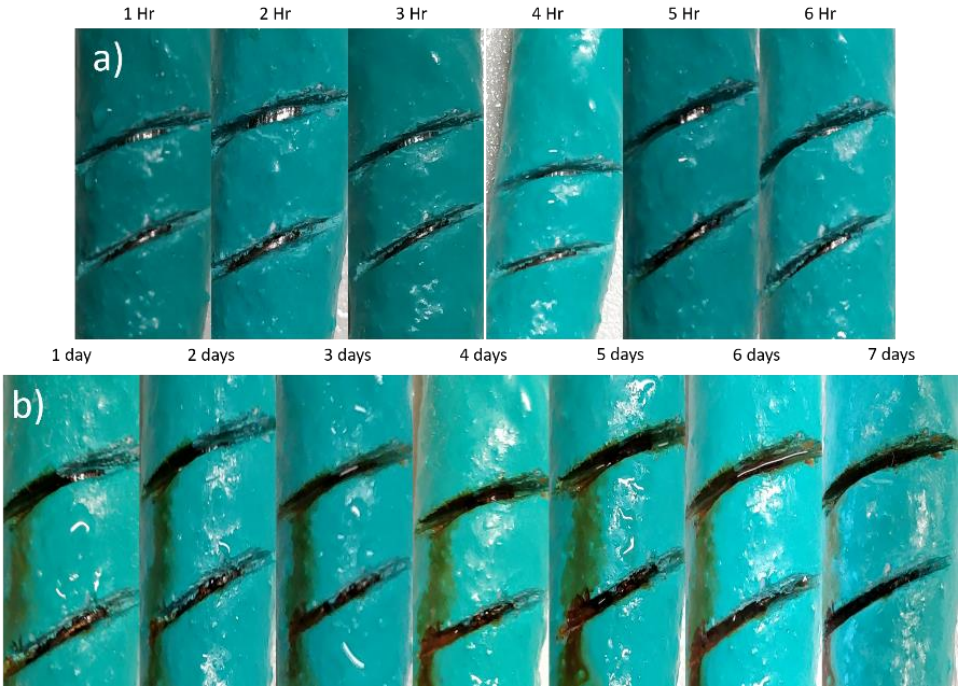

Figure 29: Exposure of C30 for a) first 6 hours of exposure, and b) 7 days inside fog chamber

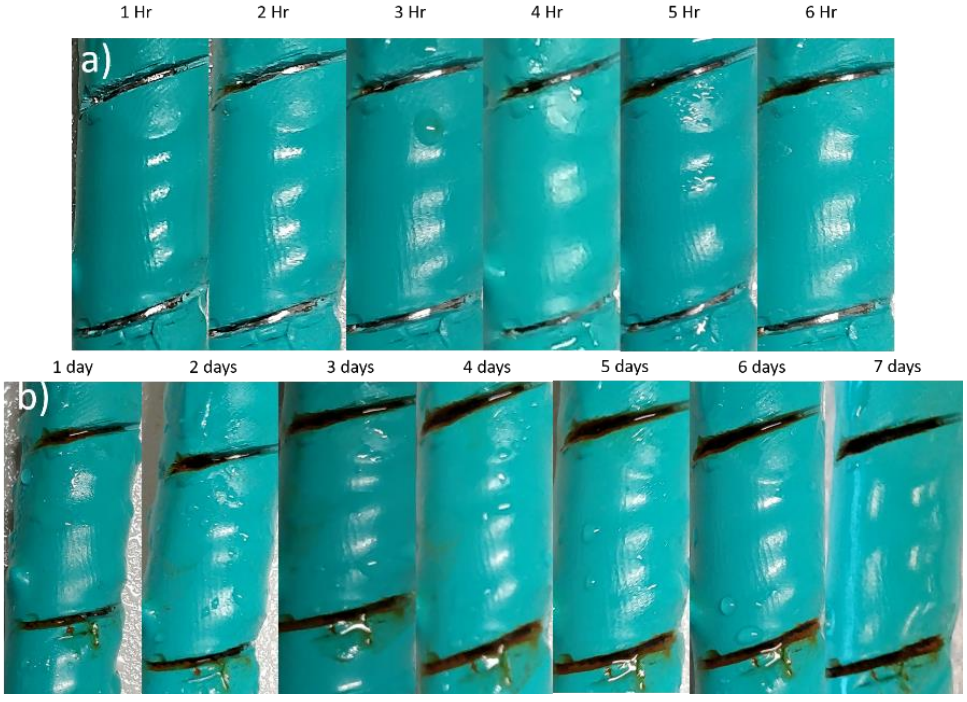

Figure 30: Exposure of Ctrl CD for a) first 6 hours of exposure, and b) 7 days inside fog chamber

3.4. SVET

From the voltage drop the current density can be calculated using [38]:

$$i = -k\frac{\Delta V}{\Delta r} = -\frac{\Delta V}{\rho \Delta r} \quad (6)$$

Where k is the solution conductivity, ρ is the solution resistance, ΔV is the potential\l difference between the substrate and probe, and Δr is the distance between the surface and probe. The solution resistance was calculated using a standard gold wire and varying the applied current and measuring the voltage drop at a fixed height above the surface. The measured current density can show if the corrosion process is occurring on the surface of the metal.

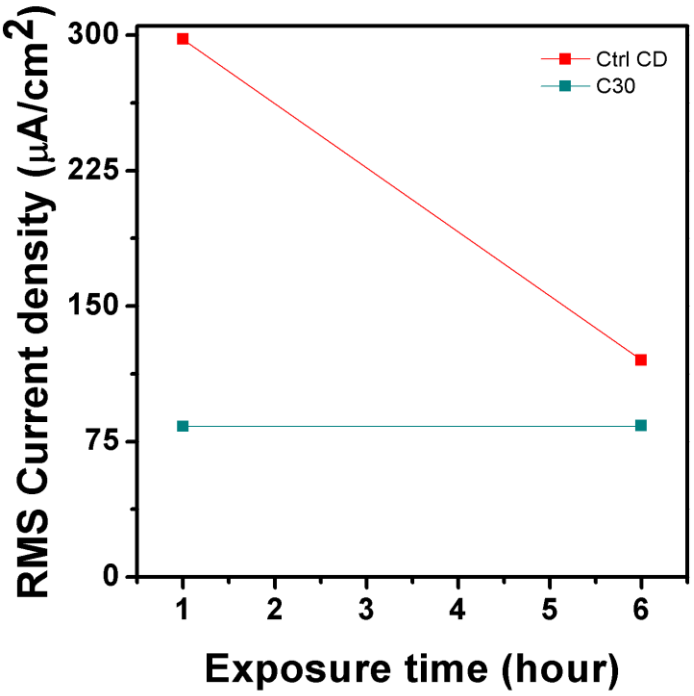

Figure 31: RMS of the current density with exposure time

In Figure 31 the root mean square (RMS) of the current densities for the two samples for varying exposure times is shown. In the first 1 hour of exposure the sample with not

microcapsules showed a large RMS due to the corrosion process occurring on the surface, this RMS value is roughly 3 times as large as the current density value for microcapsule containing coating. With increasing exposure time, the RMS of the current density of the sample with microcapsules slightly increased, while the sample with no microcapsules decreased. Even though the sample with not microcapsules decreased is was still 1.5 time larger than the sample with microcapsules. The smaller RMS value of the microcapsule sample is due to the protection layer that is formed causing smaller current peaks on the surface. These smaller current peaks correspond to a lower corrosion process occurring on the substrate. Figures 32 shows the current density of the sample C30 and Ctrl CD at 1 hour after immersion in CSPS. There were no relatively large peaks in current density on the surface between 1 and 6 hours of immersion for C30 compared to Ctrl CD. Ctrl CD showed large current peaks on the surface, and this could be due to the corrosion process occurring on the surface with nothing to lower the current like a TEA layer that is formed for C30 which has a lower current density. In Figure 33 the current density is shown for Ctrl CD and C30 for immersion times of 6 hours in CSPS. The current density was slightly increased between immersion times of 1 hour and 6 hours for C30. This rise in the current is due to the corrosion process starting on the surface, but still being limited by the formation of the TEA layer on the surface For Ctrl CD there is a decrease in the number of large current density peaks on the surface. This is possibly due to the formation of corrosion products on the surface lowering the current on the surface. The results from SVET showed the protective capabilities of TEA when the coating has been damaged and exposed to a corrosive environment. The comparison of C30 to Ctrl Cd shows that the control sample with no microcapsules showed many peaks in the current both in the anodic and cathodic direction. This difference between the

two coatings is that TEA released from the microcapsules onto the surface will lower the current density which is the same as slowing the corrosion process protecting the surface.

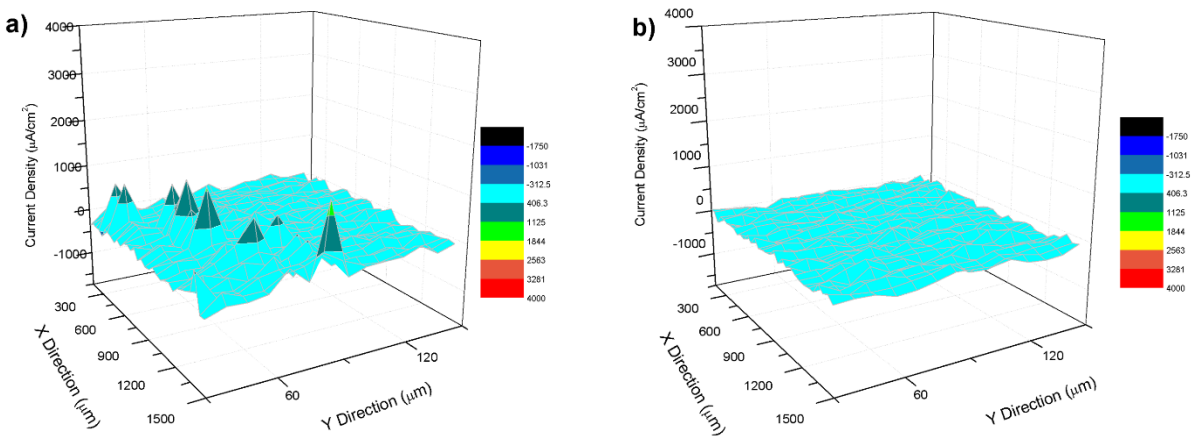

Figure 32: Current density of a) Ctrl CD, b) C30 after 1-hour exposure in carbonated simulated pore solution

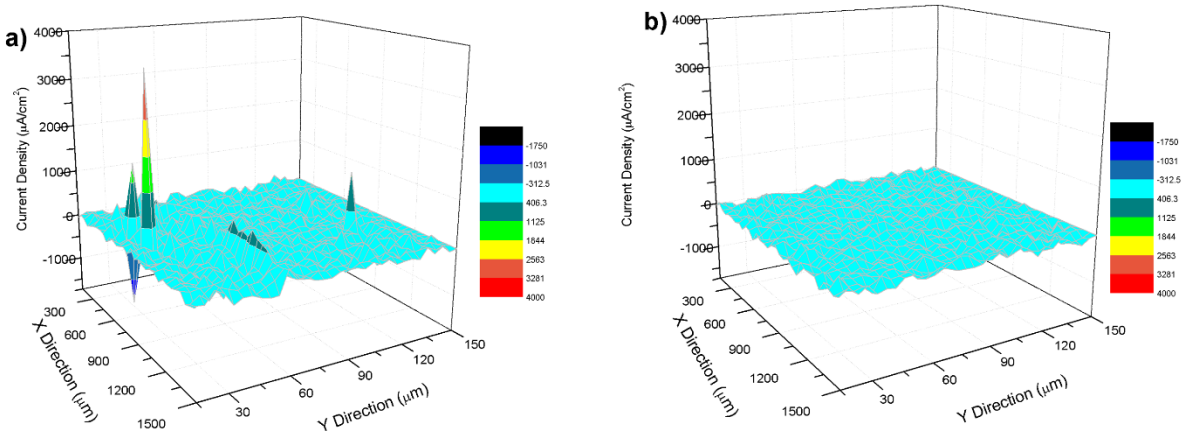

Figure 33: Current density of a) Ctrl CD, b) C30 after 6 hours exposure in carbonated simulated pore solution

3.5 SEM/EDS

Figures 34 and 35 show the results from SEM and EDS characterization of the samples after exposure in the carbonated simulated pore solution. Table 10 shows the comparison between the chemical composition between the EDS for C30 and Ctrl CD. From this testing we cannot directly determine if a TEA layer is formed on the substrate from the SEM images or the

composition obtained from EDS. The SEM does show a difference in the coverage area of corrosion products on the substrate. Ctrl CD showed was almost completely covered in corrosion products in areas where corrosion was observed, while C30 only showed a thin layer of corrosion products in certain areas. The difference in the corrosion areas of the two samples is possibly due to the formation of a TEA layer on C30 which would protect the exposed substrate. From the EDS scan it can be seen that there is a difference in the chemical compositions. Mainly there is a difference in the concentration of iron and oxygen found in the scan areas. Ctrl CD showed a much lower concentration of iron, but a higher concentration of oxygen compared to C30. This difference could be due to the amount of corrosion that has occurred in the area. For Ctrl CD the corrosion was allowed to freely occur with out inhibition, but once the corrosion process began on C30 the microcapsules in the surrounding area could release TEA to form a layer on the surface slowing down the corrosion process. Since the corrosion products typically have higher ratio of oxygen in the corrosion products it would be expected that a higher concentration of oxygen will be found in areas of corrosion.

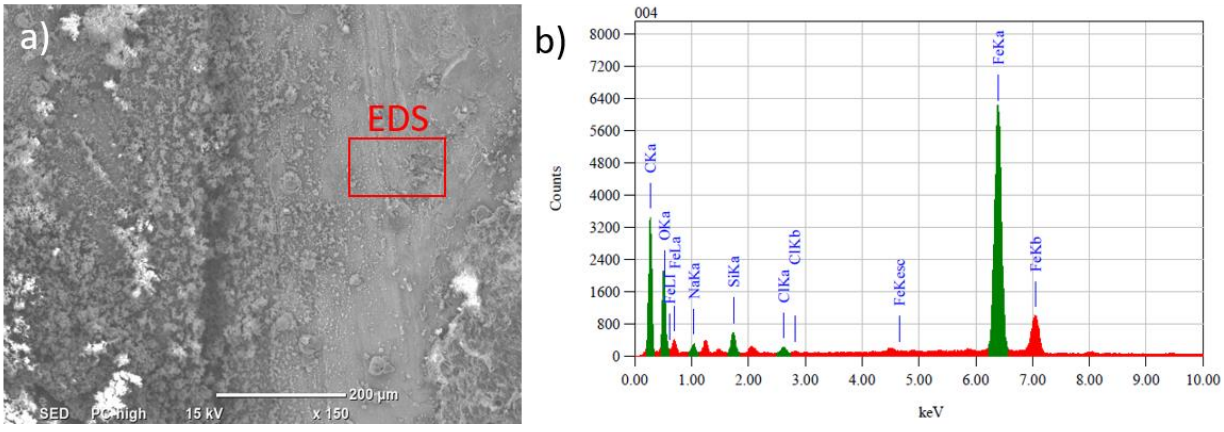

Figure 34: SEM/EDS results for C30 a) SEM micrograph at x150, b) EDS results from the measured area marked by box

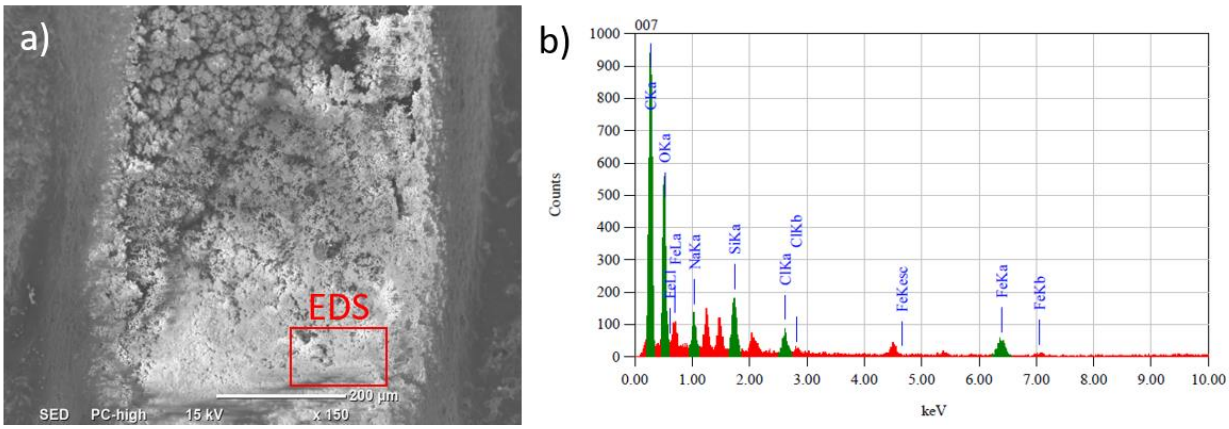

Figure 35: SEM/EDS results for Ctrl CD a) SEM micrograph at x150, b) EDS results from the measured area marked by box

Table 10: Chemical Composition of the measured EDS area by mass %

Sample	C (mass %)	O (mass %)	Na (mass %)	Si (mass %)	Cl (mass %)	Fe (mass %)
Ctrl CD	54.09	35.71	2.31	2.03	1.12	4.74
C30	29.69	8.69	0.78	0.78	0.27	59.79

From these SEM and EDS observations it can be seen that the coating with the addition of microcapsules can provide protection to the substrate after damage has occurred to the coating. This protection is most likely from a discontinuous layer that is formed on the surface which can be seen by the localized spots of corrosion on the surface of the sample with 30% microcapsules. There is most likely not a complete coverage by TEA due to there not being a high enough concentration to form a complete film.

3.6 Proposed Mechanism of Protection

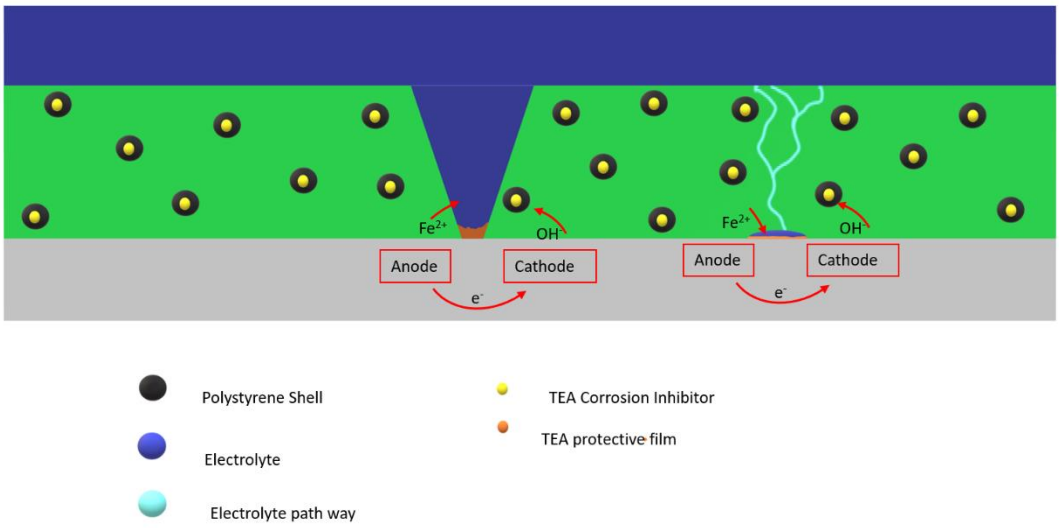

Figure 36: Release of the TEA from microcapsules in the admixed coating

Figure 36 depicts the proposed mechanism of protection of the exposed substrate by microcapsules when damage has occurred to the coating. The pH difference needed to release the TEA from the microcapsules is due to the environment formed inside areas of localized corrosion. The pH inside the pits formed are lower than the pH of the bulk environment due to the hydrolysis of the cation [33]. The formation of areas of localized corrosion can come from mechanical damage to the coating or from the diffusion of water from the environment through the coating. In these areas the corrosion process is occurring and the pH is lower than that of the bulk environment. This pH difference is the driving force for the release of the TEA to protect the exposed substrate. Once the TEA is released it will diffuse to the exposed substrate, and once at the substrate will for a protective amine layer on the surface. This layer will act as another barrier protecting the substrate even after damage has occurred to the coating.

4. SUMMARY AND CONCLUSIONS

4.1 Summary

Microcapsules containing TEA were admixed into an epoxy coating to be studied as a form of corrosion inhibition for epoxy coated rebar after the coating has become damaged. The objective of this research was to determine if there was any major effect the addition of microcapsules had an effect on the adhesion strength of the coating, and to also determine if the addition of TEA microcapsules can be used to extend the service life of the epoxy coated rebar specifically after damage has occurred to the coating. To study the inhibitive and reprotectivness of the coatings containing microcapsules were subject to mechanical and accelerated corrosion testing. To study the effect of the addition of microcapsules on the adhesion of the coating to the metal substrate three ASTM adhesion tests was performed for a qualitative ranking the coatings. Accelerated corrosion testing was performed on damaged samples to test the inhibitive properties of the TEA microcapsules admixed in the coating. Accelerated testing was performed in fog chamber at 35°C with a 5% NaCl fog and exposed for 7 days. This testing was an accelerated method to visually compare the time take for corrosion to begin on the exposed substrate as well as the time taken for the entire exposed area to become fully corroded. SVET testing is a localized electrochemical method to measure the potential difference between the exposed substrate and the SVET probe tip. The potential difference is the due to the local currents on the surface arising from the corrosion process occurring on the exposed substrate. From this testing it can be seen if some sort of protective layer is formed by a decrease in the current density measured on the surface. The surface of the exposed substrate was examined with SEM and EDS to further characterize the corrosion inhibition properties of the addition of TEA filled microcapsules. A TEA layer cannot be directly seen from these methods but a difference in the

area covered by corrosion products and a difference in composition measured by EDS can be seen. Global electrochemical testing was performed in carbonated simulated pore solution to further characterize the corrosion inhibition effect from the addition of microcapsules. The global electrochemical tests run are; open circuit potential, linear polarization resistance, and electrochemical impedance spectroscopy. These tests allow a chance to measure the properties of the coating along with the effect of the addition of microcapsules.

4.2 Conclusions

Based on the results from the mechanical and accelerated corrosion testing the following conclusions can be drawn. With the addition of microcapsules into the epoxy resin there is a decrease in the adhesion strength of the coating. This is most likely due to the increase in the viscosity of the epoxy resin, and the quicker curing time due to this addition.

From the electrochemical testing in carbonated simulated pore solution the open circuit potential, polarization resistance calculated from linear polarization resistance, and electrochemical impedance spectroscopy are used to compare the coated samples. The OCP values for all samples tested all fell into range of -535 mV vs SCE to -645 mV vs SCE, which from ASTM C876 shows a greater than 90% probability of corrosion occurring on the rebar [39]. The polarization resistance of all coated samples decreased with immersion time. Which is possibly from the corrosion process occurring on the exposed surface with exposure time. The polarization resistance measured was larger for the duration of exposure for the samples with the addition of microcapsules. It was also shown that the addition of microcapsules increased the low frequency bode value and kept it higher than the sample with no microcapsules for the duration of testing. In the high to middle frequencies the coatings with microcapsules showed a more capacitive response with higher phase angle values and a shorter plateau at higher

frequencies than the control sample. Which could be due to the formation of TEA layer on the exposed rebar.

From SVET the samples containing TEA microcapsules show a large decrease in the current recorded compared to that of the control samples during immersion. This drop in the measure potential is possibly due to the formation of a TEA layer on the surface which would lower the potential difference measured between the SVET probe tip and exposed substrate. SEM and EDS measurements showed a difference in the damaged coating area after exposure. From SEM it can be seen that there is a difference in the coverage area of corrosion products on the surface, the sample with no microcapsules showed an almost complete coverage in the area that exhibited corrosion, while the sample with microcapsules only showed small localized areas of corrosion on the substrate. EDS of measurements on the surface showed a large difference in the amount oxygen and iron measured on the surface. The sample with microcapsules showed a large iron concentration and low oxygen concentration while the sample with no microcapsules showed the opposite. This could be due the larger amount of corrosion products formed on the sample with no microcapsules while there was still exposed substrate for the sample with microcapsules in the coating.

The addition of microcapsules containing TEA demonstrated an inhibitive effect that protected the rebar once damaged has occurred to the coating exposing the substrate. It has been shown that addition of TEA encapsulated in polymeric shells and admixed into epoxy coating can provide a corrosion inhibition effect in damaged coating extending its service life without large adverse effects to the mechanical properties of the coating.

REFERENCES

1. Hartt, W.H., R. G. Powers, V. Leroux, and D. K. Lysogorski, *Critical Literature Review of High-Performance Corrosion reinforcements in Concrete Bridge Applications: Final Report.* Fhwa-Hrt-04-093, 2004.
2. Tuutti, K., *Corrosion of Steel in Concrete*. Materials Engineering. 1982, Stockholm: Swedish Cement and Concrete Research Institute. 468.
3. Grubb, J.A., H.S. Limaye, and A.M. Kakade, *Testing pH of Concrete.* Concrete International, 2007. **29**(4).
4. Böhni, H., *Corrosion in reinforced concrete structures*. 2005, Cambridge, England Boca Raton: Woodhead; CRC Press. xiv, 248 p.
5. Angst, U.M., et al., *Chloride Induced reinforcement corrosion: electrochemical monitoring of initiation stage and chloride threshold values.* Corrosion Science, 2011. **53**(4): p. 1451-1464.
6. Alonso, C., et al., *Chloride threshold values to depassivate reinforcing bars embedded in a standardized OPC mortar.* Cement and Concrete research, 2000. **30**(7): p. 1047-1055.
7. Broomfield, J.P., *Corrosion of steel in concrete: Understanding, investigation and repair*. 2007, London: Taylor & Francis.
8. Bremner, T., et al., *Protection of Metals in Concrete Against Corrosion.* 2001.
9. Pedeferri, P., *Cathodic Protection and cathodic prevention.* Construction and Building Materials, 1996. **10**(5): p. 391-402.
10. Söylev, T.A. and M.G. Richardson, *Corrosion inhibitors for steel in concrete: State-of-the-art report.* Construction and Building Materials, 2008. **22**(4): p. 609-622.
11. Gaidis, J.M., *Chemistry of corrosion inhibitors.* Cement and Concrete Composites, 2004. **26**(3): p. 181-189.
12. De Schutter, G. and L. Luo, *Effect of corrosion inhibiting admixtures on concrete properties.* Construction and Building Materials, 2004. **18**(7): p. 483-489.
13. Brown, M.C., R.E. Weyers, and M.M. Sprinkel, *Effect of corrosion-inhibiting admixtures on material properties of concrete.* Materials Journal, 2001. **98**(3): p. 240-250.
14. Gustafson, D., *Epoxy Update.* Civil Engineering, 1988. **58**.
15. Smith, L.L., Kessler, R.J., Powers, R.G. , *Corrosion of epoxy-coated rebar in a marine environment.* Transportation Research Board, 1993(403): p. 36-45.
16. Virmani, Y.P. and G.G. Clemena, *Corrosion protection: Concrete bridges*. 1998, United States. Federal Highway Administration.
17. ASTM, *ASTM A775/ A775M-17*, in *Standard Specification for Epoxy-Coated Steel Reinforcing Bars*. 2017, ASTM International: West Conshohocken, PA.
18. Choi, H., Song. Y.K., Kim, K.Y., and Park, J.M., *Encapsulation of triethanolamine as organic corrosion inhibitor into nanoparticles and its active corrosion protection for steel sheets.* Surface Coatings Technology, 2012. **206**(8-9): p. 2354-2362.
19. Castaneda, H., M. Hassan, and M. Radovic, *Characterizing and understanding self-healing microcapsules embedded in reinforced structures exposed to corrosive environments* 2018.
20. *ASTM D3359-17 Standard Test Methods for Rating Adhesion by Tape Test*. 2017, ASTM International: West Conshocken, PA.
21. *ASTM D2197-16 Standard Test Method for Adhesion of Organic Coatings by Scrape Adhesion* 2016, ASTM International: West Conshocken, PA.

22. International, A., *ASTMD D4541-17 Standard Test Method for Pull-Off Strength of Coatings Using Portable Adhesion Tester`*. 2017, ASTM International: West Conshocken, PA.
23. Williamson, J. and O.B. Isgor, *The effect of simulated concrete pore solution composition and chlorides on the electronic properties of passive films on carbon steel rebar.* Corrosion Science, 2016. **106**: p. 82-95.
24. Volpi, E., et al., *Electrochemical characterization of mild steel in alkaline solutions simulating concrete environment.* Journal of Electroanalytical Chemistry, 2015. **736**: p. 38-46.
25. Moser, R.D., et al., *Chloride-induced corrosion resistance of high-strength stainless steels in simulated alkaline and carbonated concrete pore solutions.* Corrosion Science, 2012. **57**: p. 241-253.
26. Dong, B., et al., *Electrochemical impedance study on steel corrosion in the simulated concrete system with a novel self-healing microcapsule.* Construction and Building Materials, 2014. **56**: p. 1-6.
27. Alvarez, S.M., A. Bautista, and F. Velasco, *Corrosion behaviour of corrugated lean duplex stainless steels in simulated concrete pore solutions.* Corrosion Science, 2011. **53**(5).
28. Bertolini, L., et al., *Behaviour of stainless steel in simulated concrete pore solution.* British Corrosion Journal, 1996. **31**(3): p. 218-222.
29. Simpson, V., *Fundamental studies of adhesion.* 1997.
30. Pourbaix, M., *Lectures on electrochemical corrosion*. 2012: Springer Science & Business Media.
31. Davies, D. and G.J.C. Burstein, *The effects of bicarbonate on the corrosion and passivation of iron.* 1980. **36**(8): p. 416-422.
32. *ASTM C876-15 Standard Test Method for Corrosion Potentials of Uncoated Reinforcing Steel in Concrete*. 2015, ASTM International: West Conshocken, PA.
33. Mcafferty, E., *Introduction to corrosion science*. 2016: Springer.
34. Arenas, M., R.J.J.o.M. Reddy, and M.B. Metallurgy, *Corrosion of steel in ionic liquids.* 2003. **39**(1-2): p. 81-91.
35. Lamaka, S.V., et al., *Nanoporous titania interlayer as reservoir of corrosion inhibitors for coatings with self-healing ability.* 2007. **58**(2-3): p. 127-135.
36. Hsieh, G., et al., *Experimental limitations in impedance spectroscopy: Part I—simulation of reference electrode artifacts in three-point measurements.* 1996. **91**(3-4): p. 191-201.
37. Mansfeld, F., M. Kendig, and S.J.C. Tsai, *Evaluation of corrosion behavior of coated metals with AC impedance measurements.* 1982. **38**(9): p. 478-485.
38. Bastos, A., et al., *On the Application of the Scanning Vibrating Electrode Technique (SVET) to Corrosion Research.* 2017. **164**(14): p. C973-C990.
39. *Standard Test Method for Corrosion Potentials of Uncoated Reinforcing Steel in Concrete*.